

# Astrophysical Objects

## Basics of Radio astronomy

Based on Chapter 3 of Essential Radio astronomy

**Helga Dénés 2023 S2 Yachay Tech**  
[hdenes@yachaytech.edu.ec](mailto:hdenes@yachaytech.edu.ec)



**SCHOOL OF  
PHYSICAL SCIENCES  
AND NANOTECHNOLOGY**

# Radio telescopes

The radio band is too wide (five decades in wavelength) to be covered effectively by a single telescope design. The surface brightnesses and angular sizes of radio sources span an even wider range, so a combination of single telescopes and aperture-synthesis interferometers are needed to detect and image them.

The ideal radio telescope should have a **large collecting area** to detect faint sources.

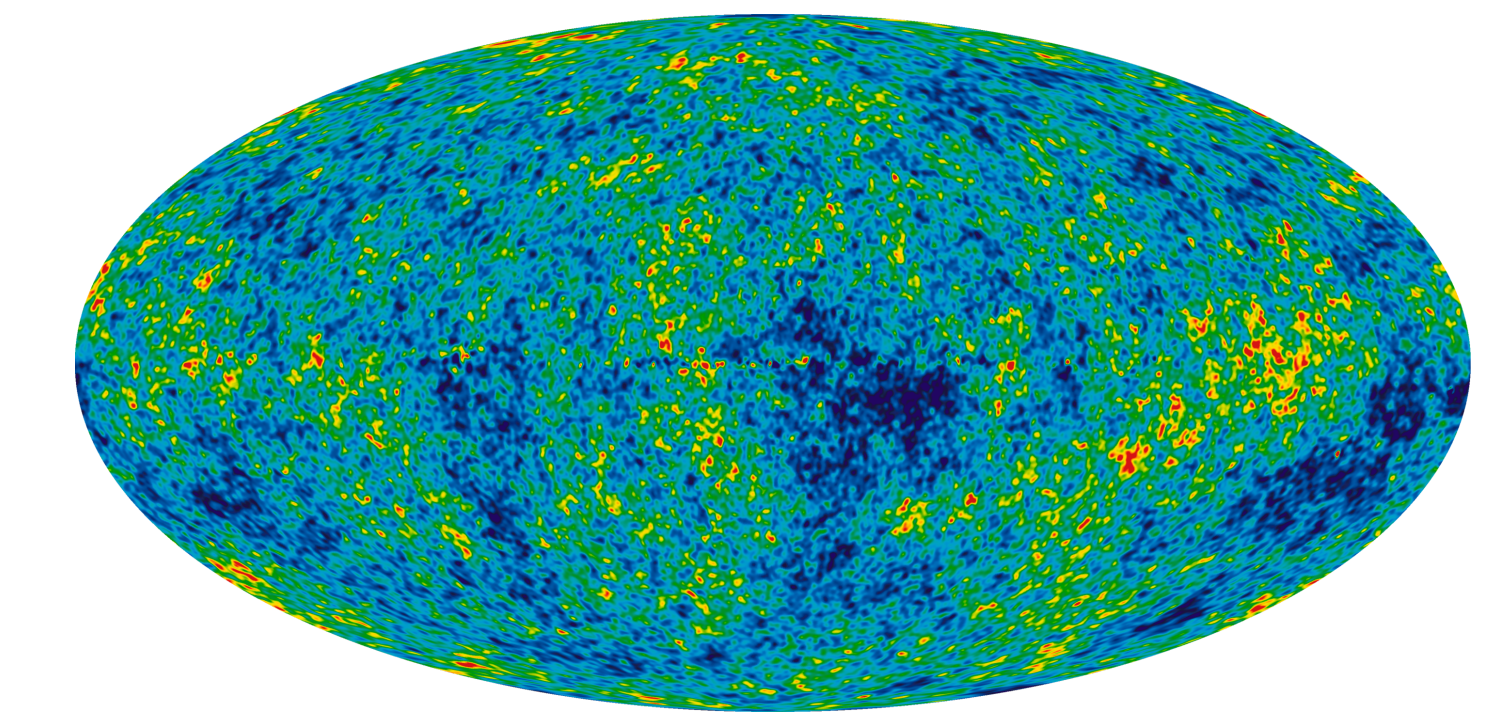
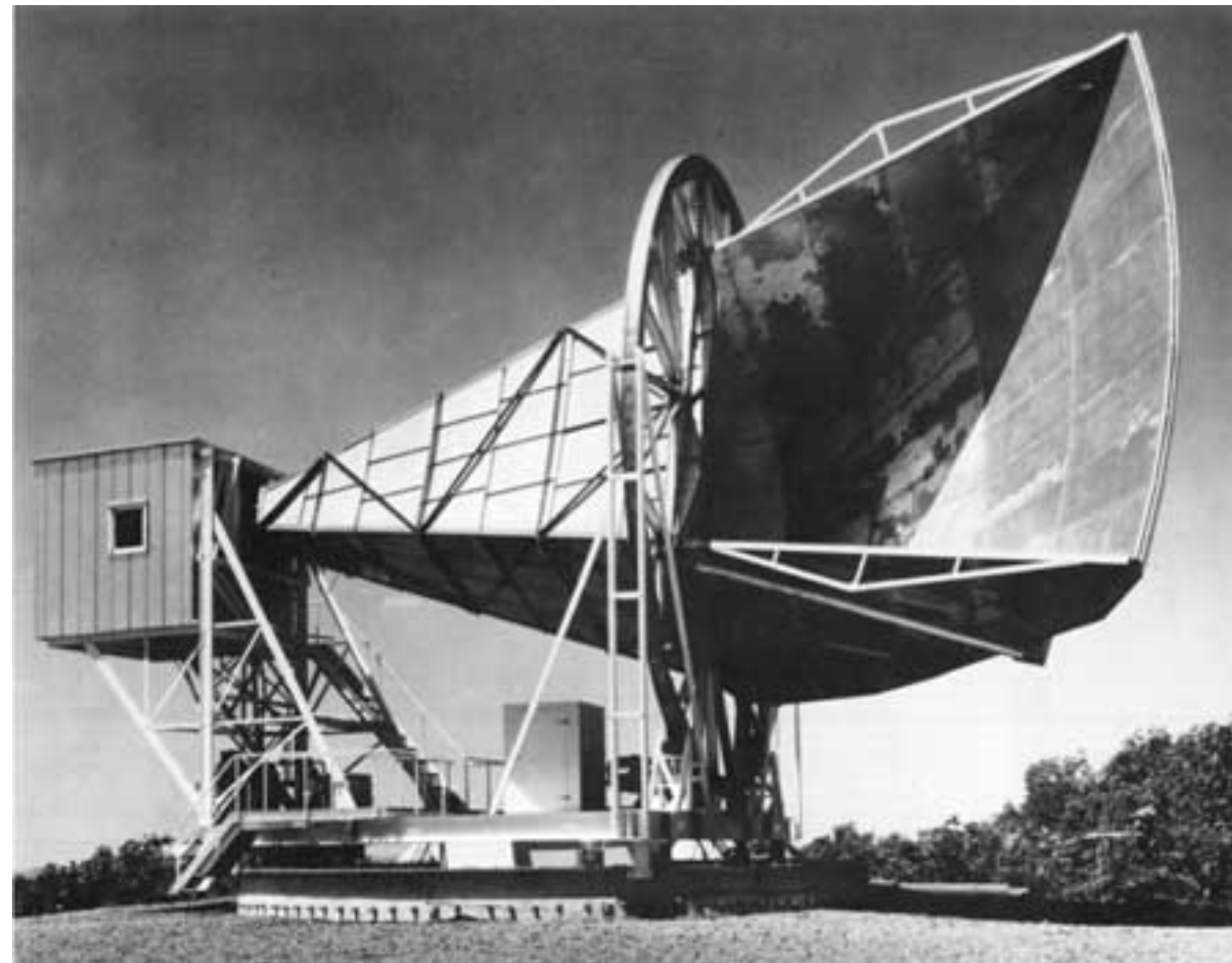
The effective collecting area  $A_e(\theta, \phi)$  of any antenna averaged over all directions  $(\theta, \phi)$  is  $A_e = \frac{\lambda^2}{2\pi}$  so large peak collecting areas imply extremely directive antennas at short wavelengths. Only at long wavelengths ( $\lambda > 1$  m) is it feasible to construct sensitive antennas from reasonable numbers of small, nearly isotropic elements such as dipoles.

The **simplest aperture antenna** is a **waveguide horn**. Radiation incident on the opening is guided by a tapered waveguide. At the narrow end of the tapered horn is a waveguide with parallel walls, and inside this waveguide is a quarter-wave ground-plane vertical antenna that converts the electromagnetic wave into an electrical current that is sent to the receiver via a cable.

# Radio telescopes

Horn antennas pick up very little ground radiation because, unlike most paraboloidal dishes, their apertures are not partially blocked by external feeds and feed-support structures, which scatter ground radiation into the receiver.

This freedom from ground pickup allowed Penzias and Wilson to show that the zenith antenna temperature of the Bell Labs horn (Figure) was 3.5 K higher at  $\nu \approx 4$  GHz than expected—the first detection of the **cosmic microwave background radiation**.



Nine-year Wilkinson Microwave Anisotropy Probe heat map of temperature fluctuations in the cosmic microwave background

The **horn antenna** at Bell Labs, Holmdel, NJ used by Penzias and Wilson to discover the 3 K cosmic microwave background radiation in 1965

# Radio telescopes

The aperture of a waveguide horn is not blocked by any feed-support structure, so it is also easier to calculate the gain of a horn antenna from first principles than to calculate the gain of a partially blocked reflecting antenna. Thus small horn antennas have been used by radio astronomers to measure the **absolute flux densities** of very strong sources such as Cas A.

Radio astronomers observing with large dishes typically do not measure the absolute flux densities of sources, only their **relative flux densities** by comparison with secondary calibration sources whose flux densities relative to that of Cas A are known in advance.

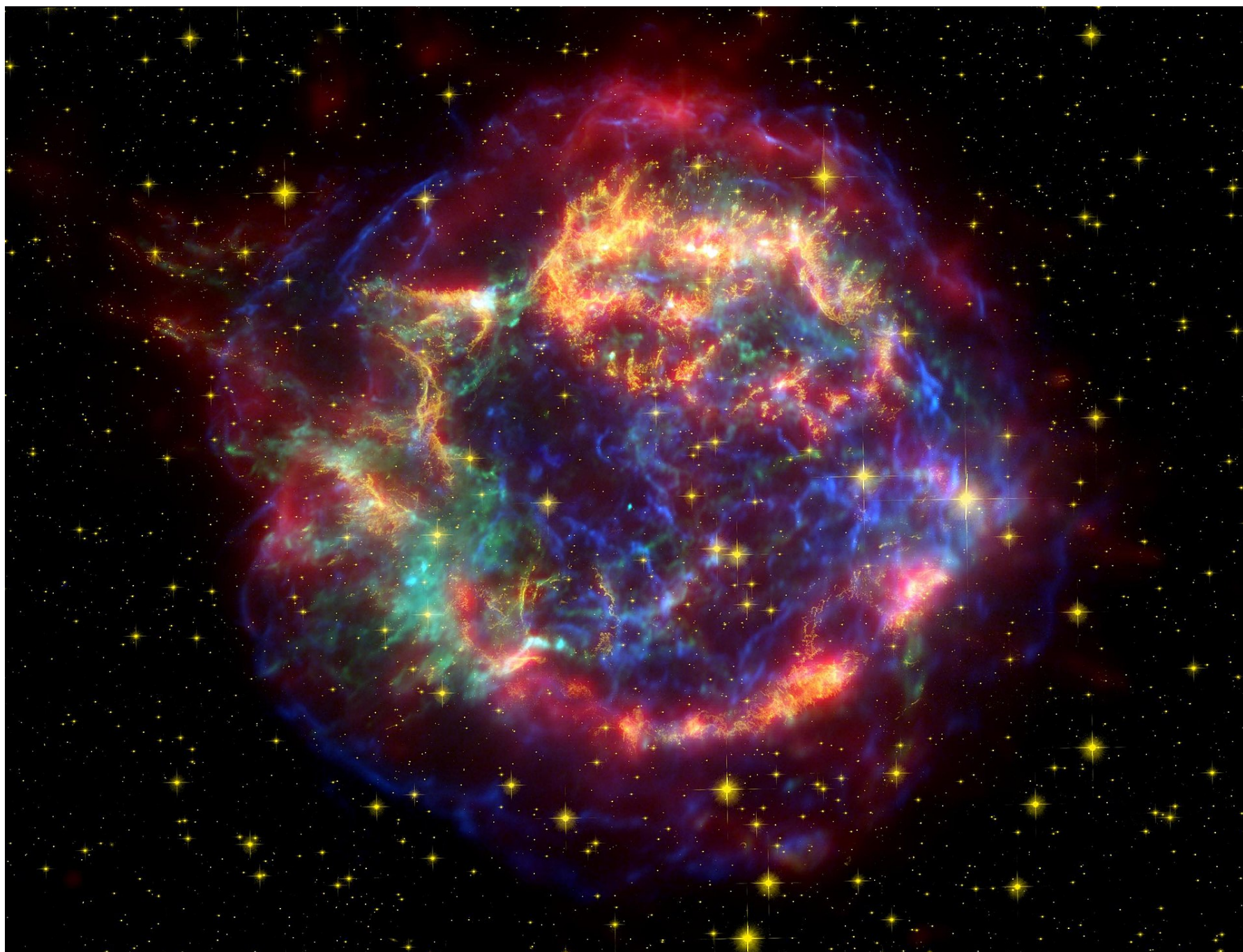


The horn antenna at Bell Labs, Holmdel, NJ used by Penzias and Wilson to discover the 3 K cosmic microwave background radiation in 1965

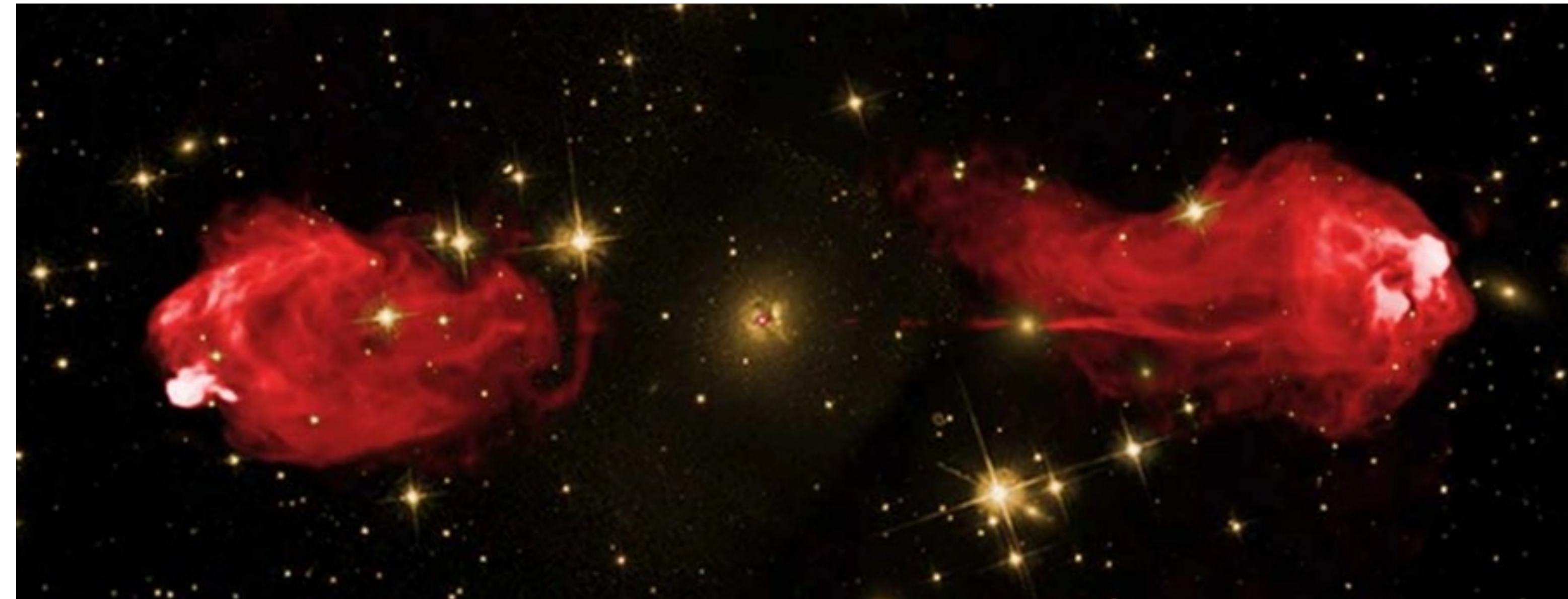
# Calibration

**Absolute flux density:** measuring the absolute flux densities of strong sources such as Cas A and Cyg A and defining the practical flux-density scales used by radio astronomers

Cas A - Supernova remnant



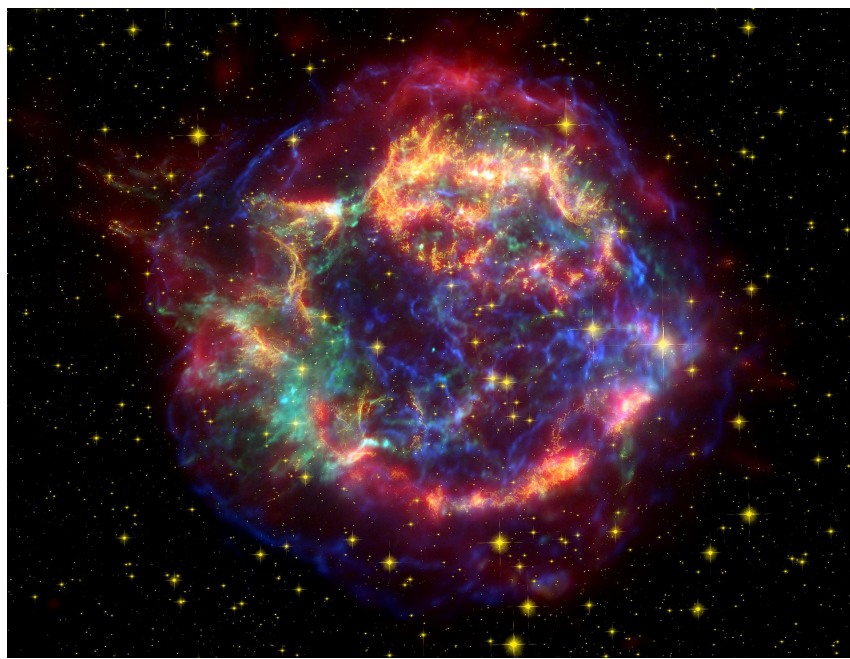
Cyg A - radio galaxy (AGN)



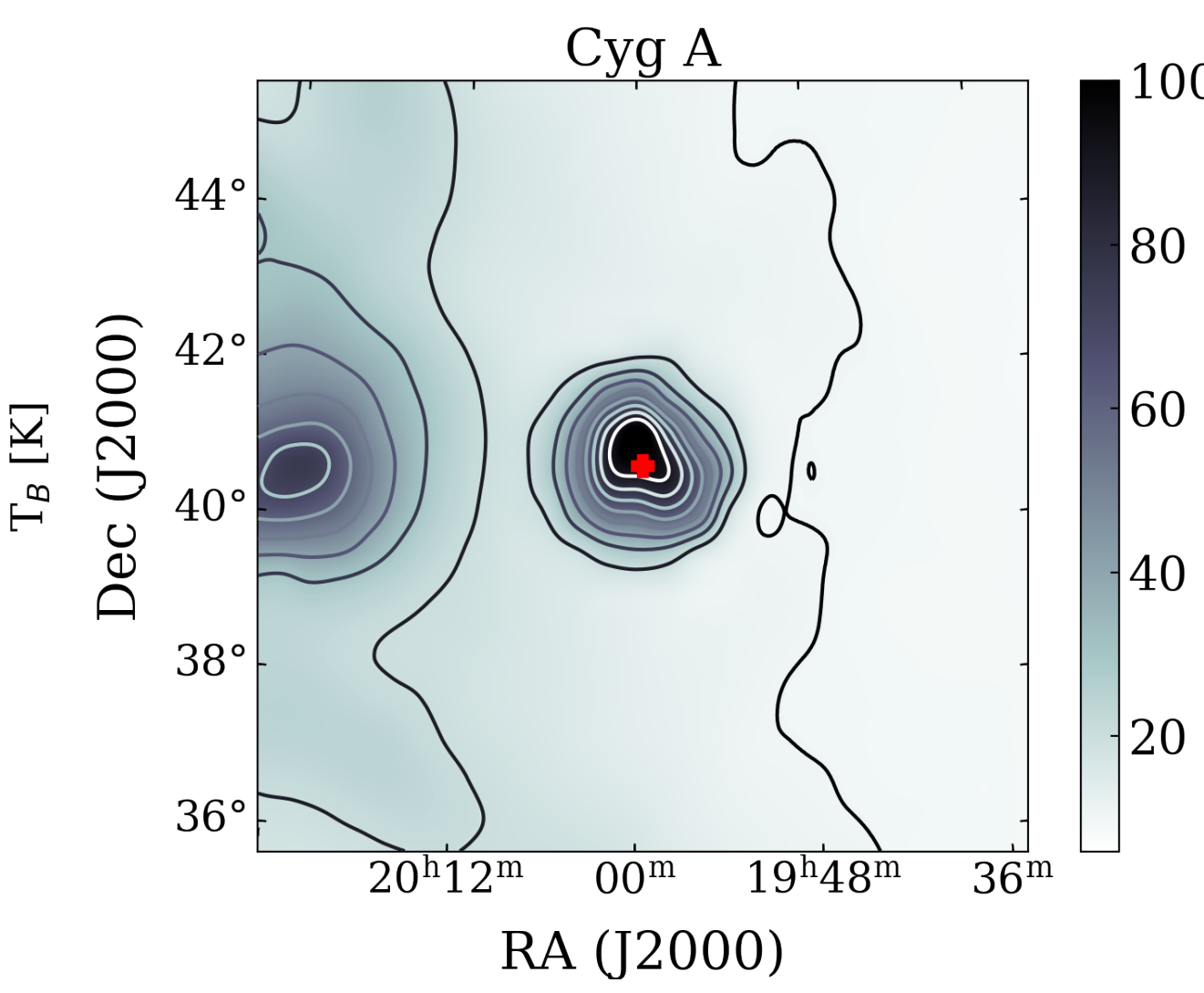
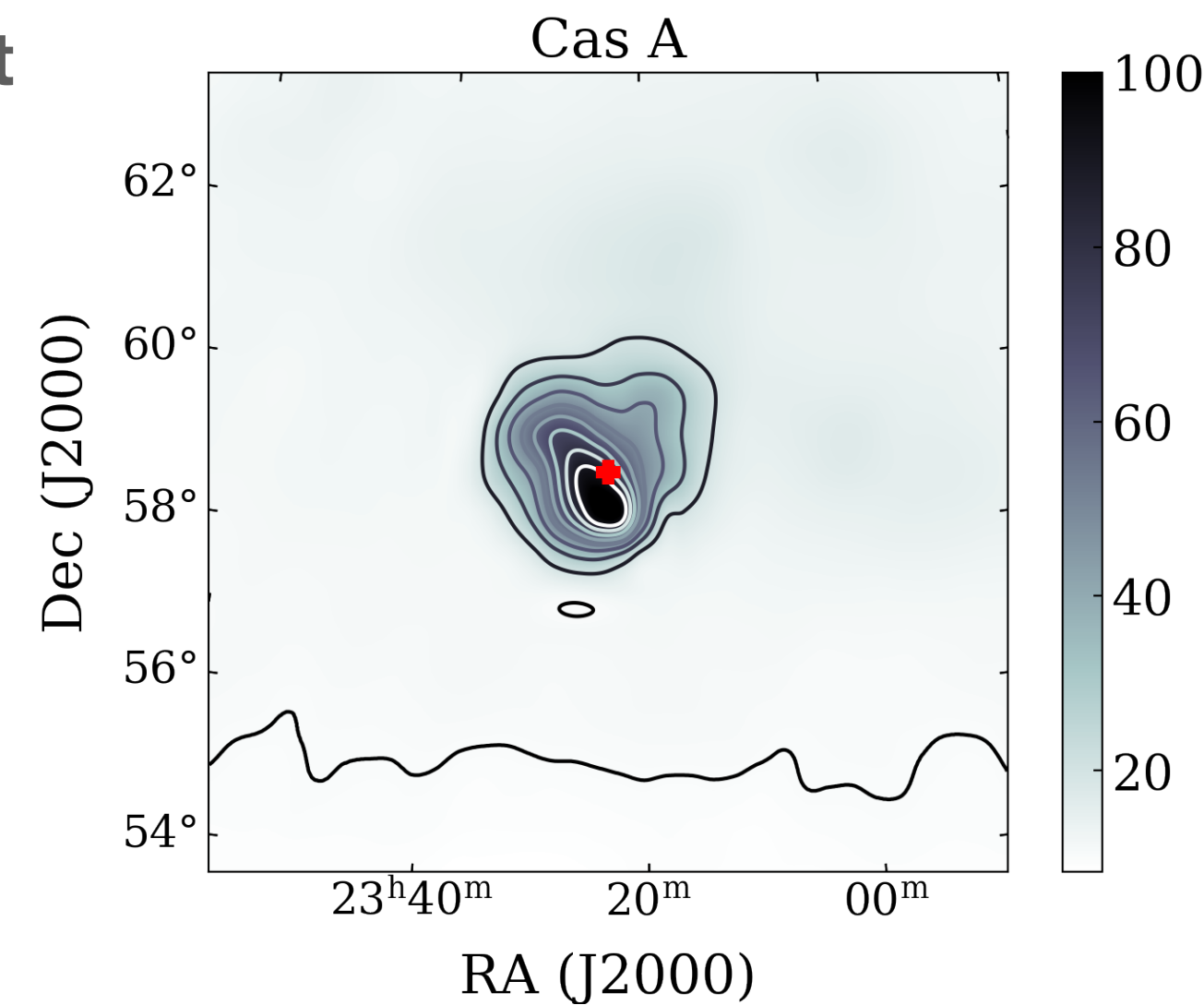
# Calibration

**Absolute flux density:** measuring the absolute flux densities of strong sources such as Cas A and Cyg A and defining the practical flux-density scales used by radio astronomers

Cas A - Supernova remnant



Cas A and Cyg A with the Dwingeloo telescope at 21 cm



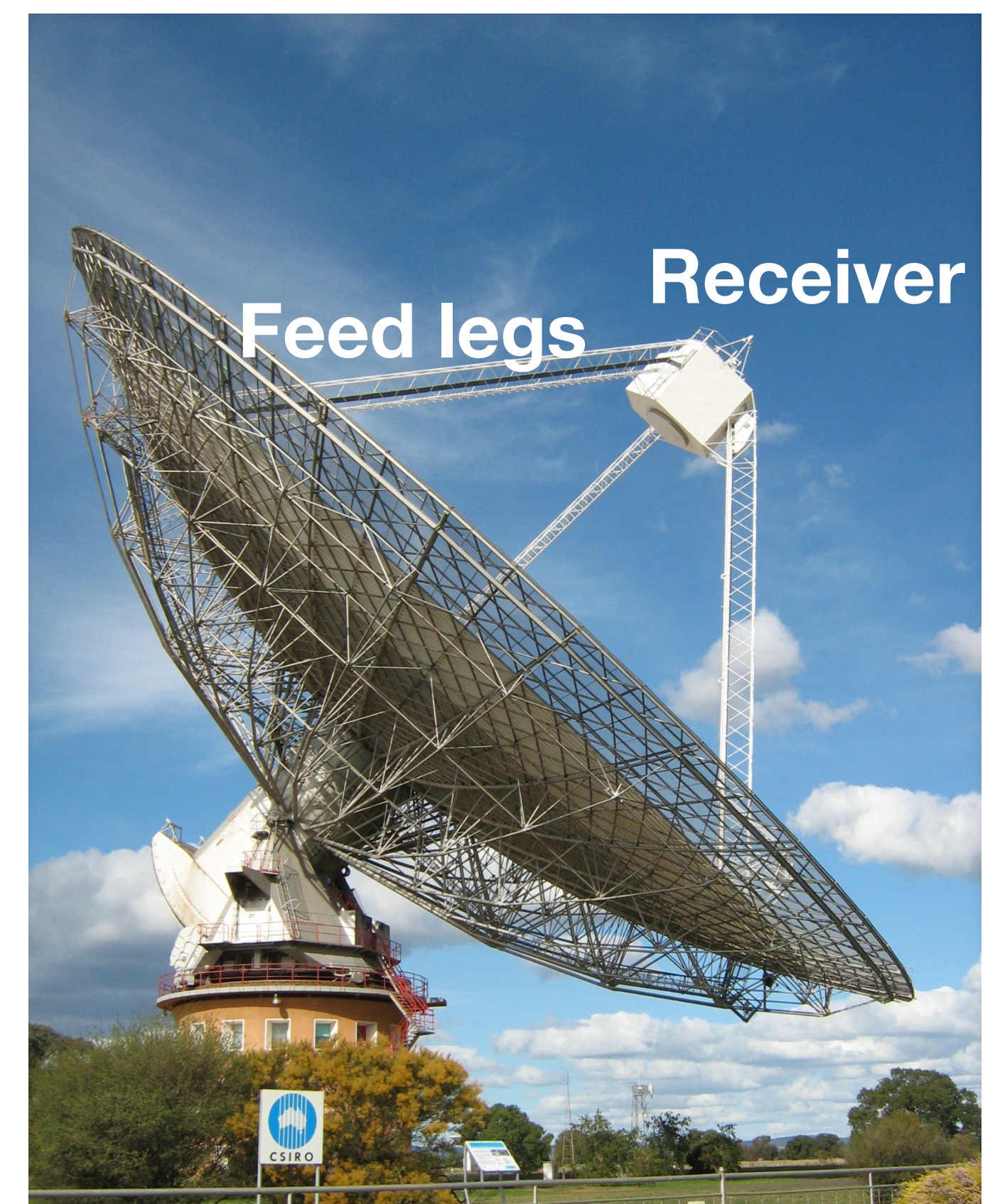
Cyg A - radio galaxy (AGN)



# Radio telescopes

Most radio telescopes use circular paraboloidal reflectors to obtain large collecting areas and high angular resolution over a wide frequency range. Because the feed is on the reflector axis, the feed and legs supporting it partially block the path of radiation falling onto the reflector. This **aperture blockage** has a number of undesirable consequences:

1. The effective collecting area is reduced because some of the incoming radiation is blocked.
2. The beam pattern is degraded by increased sidelobe levels.
3. Radiation from the ground that is scattered off the feed and its support structure increases the system noise.
4. Radiation from the Sun and artificial sources of radio frequency interference (RFI) far from the main beam will be mixed with the desired signal.

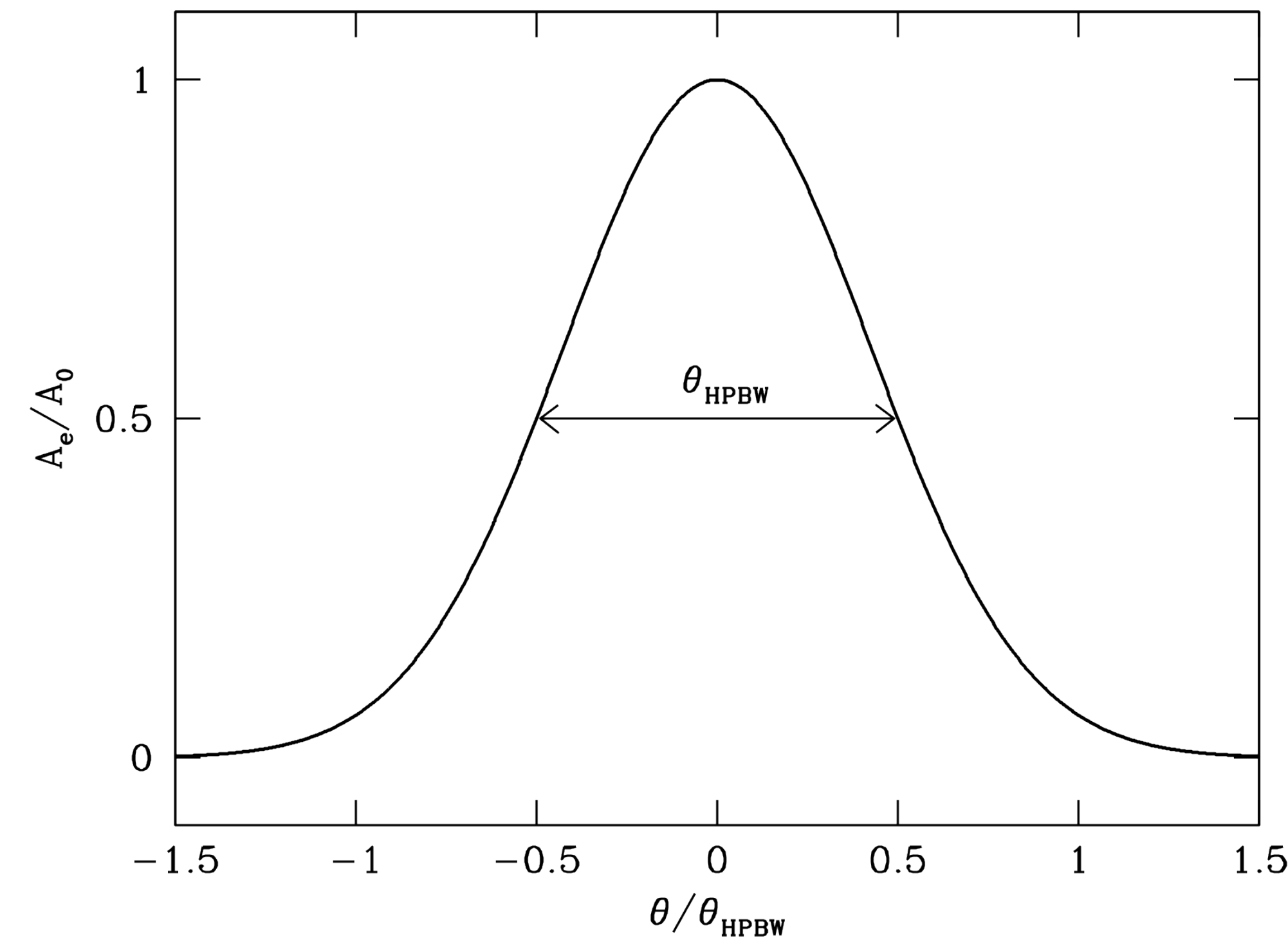


# Gaussian Beam Solid Angle and Beamwidth

Most apertures associated with reflectors and lenses are circular. The power pattern of a uniformly illuminated circular aperture is known as the **Airy pattern**.

Figure 3.15: The beams of most radio telescopes are nearly Gaussian, and their beamwidths are usually specified by the angle  $\Theta_{HPBW}$  between the half-power points.

Abscissa: offset  $\theta$  from the beam center in units of the HPBW. Ordinate: Effective aperture  $A_e$  normalized by the peak effective aperture  $A_0$



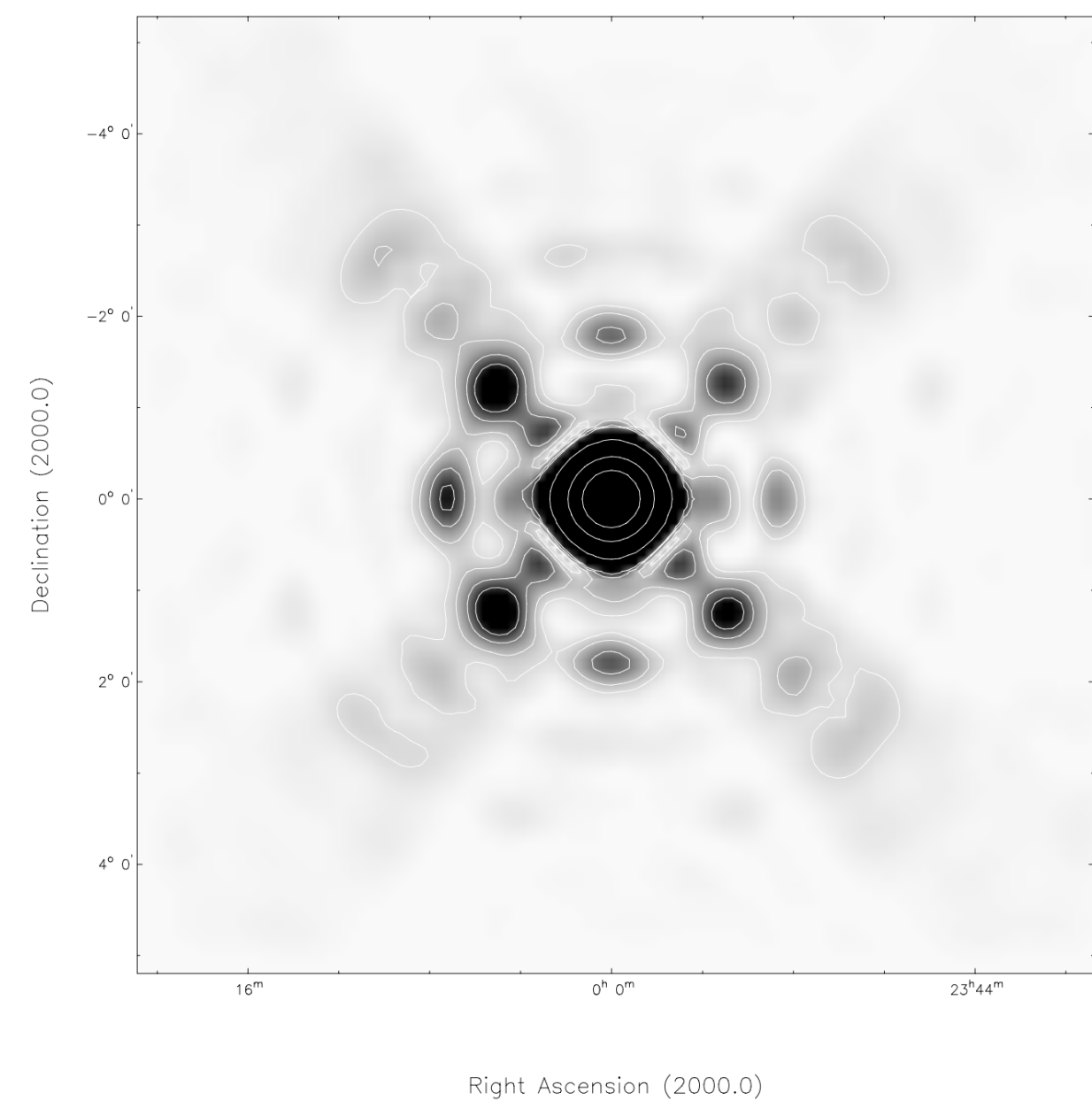
the beam solid angle of a Gaussian beam is:

$$\Omega_A = \left( \frac{\pi}{4 \ln 2} \right) \theta_{HPBW}^2 \approx 1.133 \theta_{HPBW}^2$$

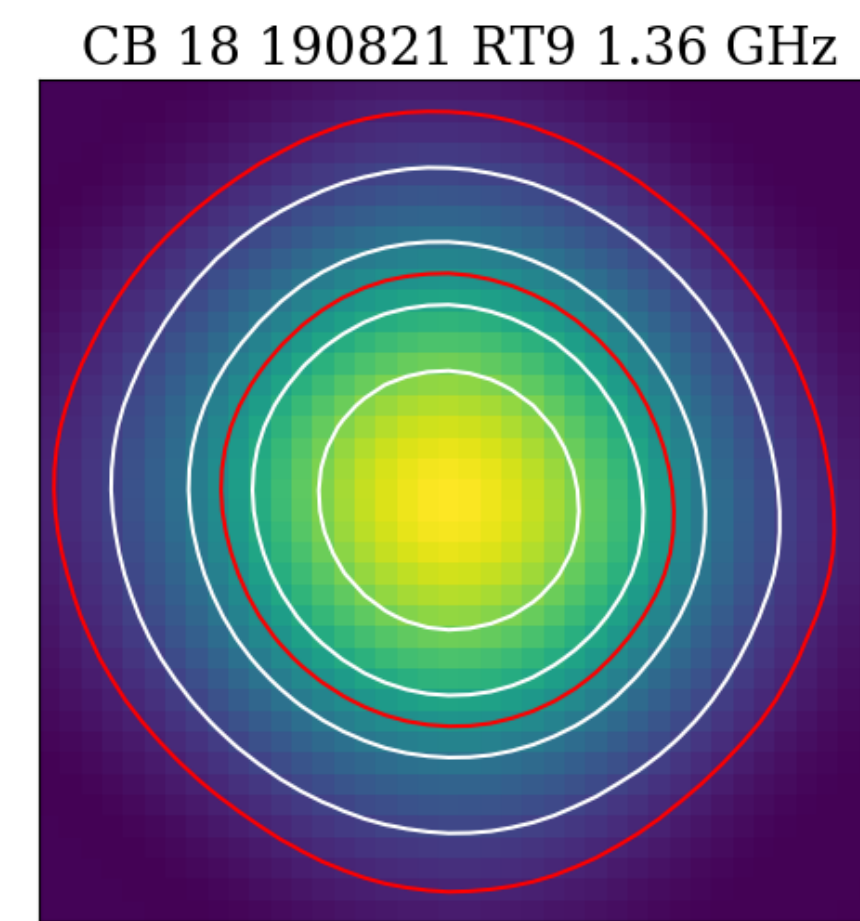
# Gaussian Beam

- The primary beam response is important for
  - Correct deconvolution of the images
  - Correct flux scale**
  - Mosaicking

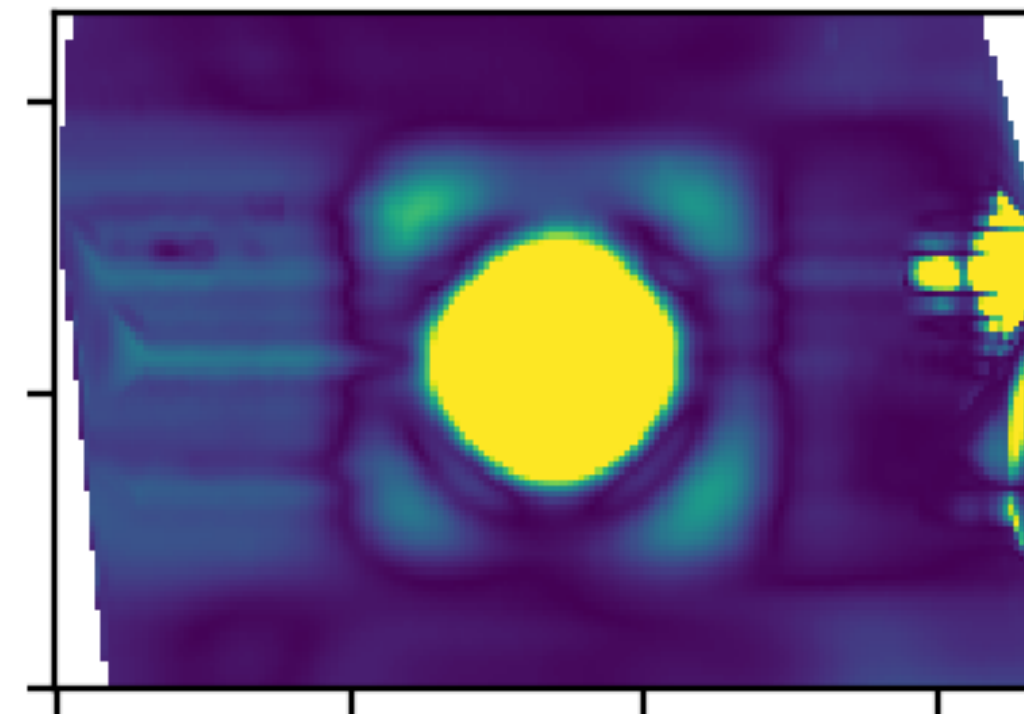
WSRT beam shape from Popping et al. 2008



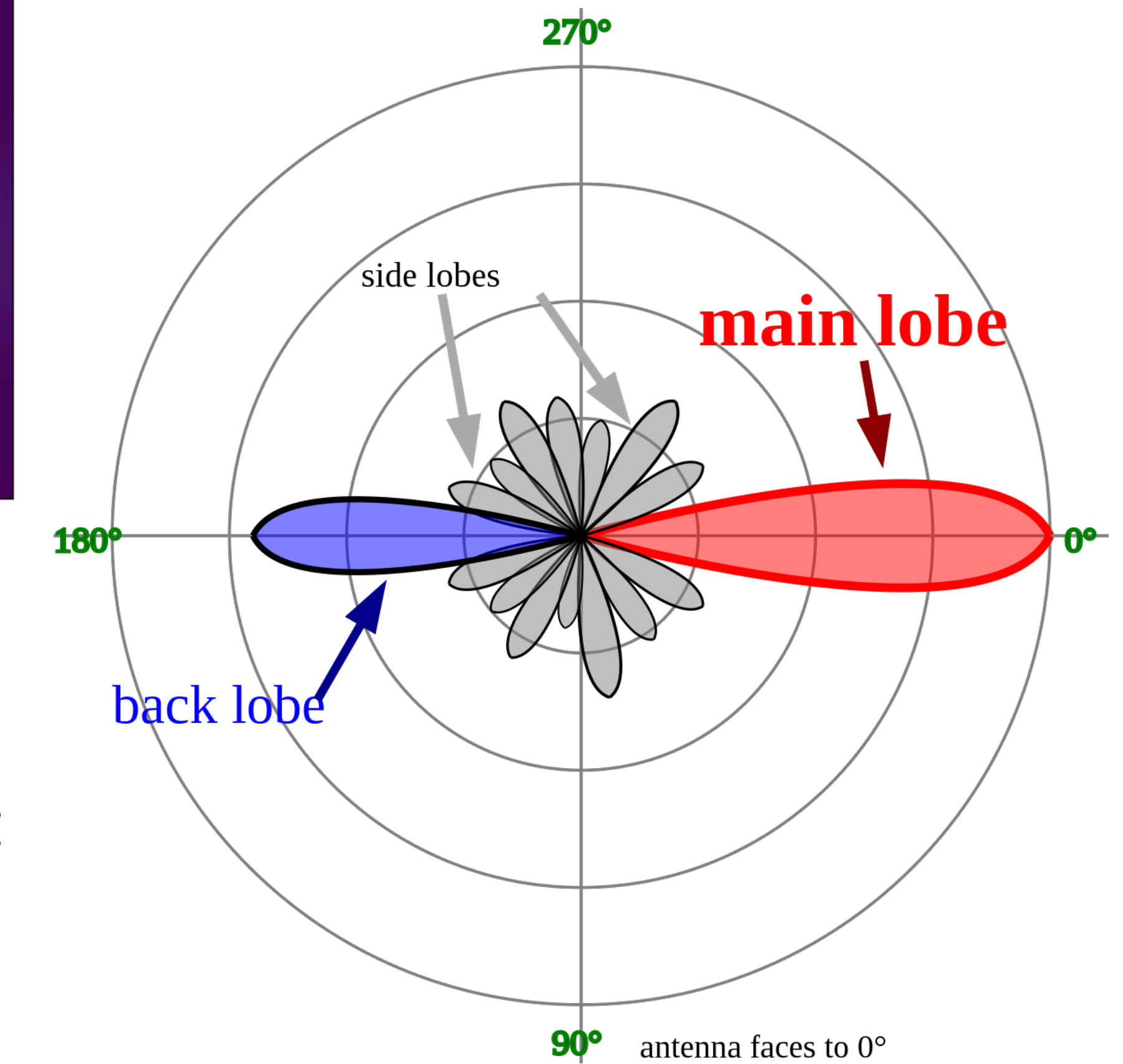
Primary beam pattern



Faint side lobes



Antenna radiation pattern



# Radio telescopes

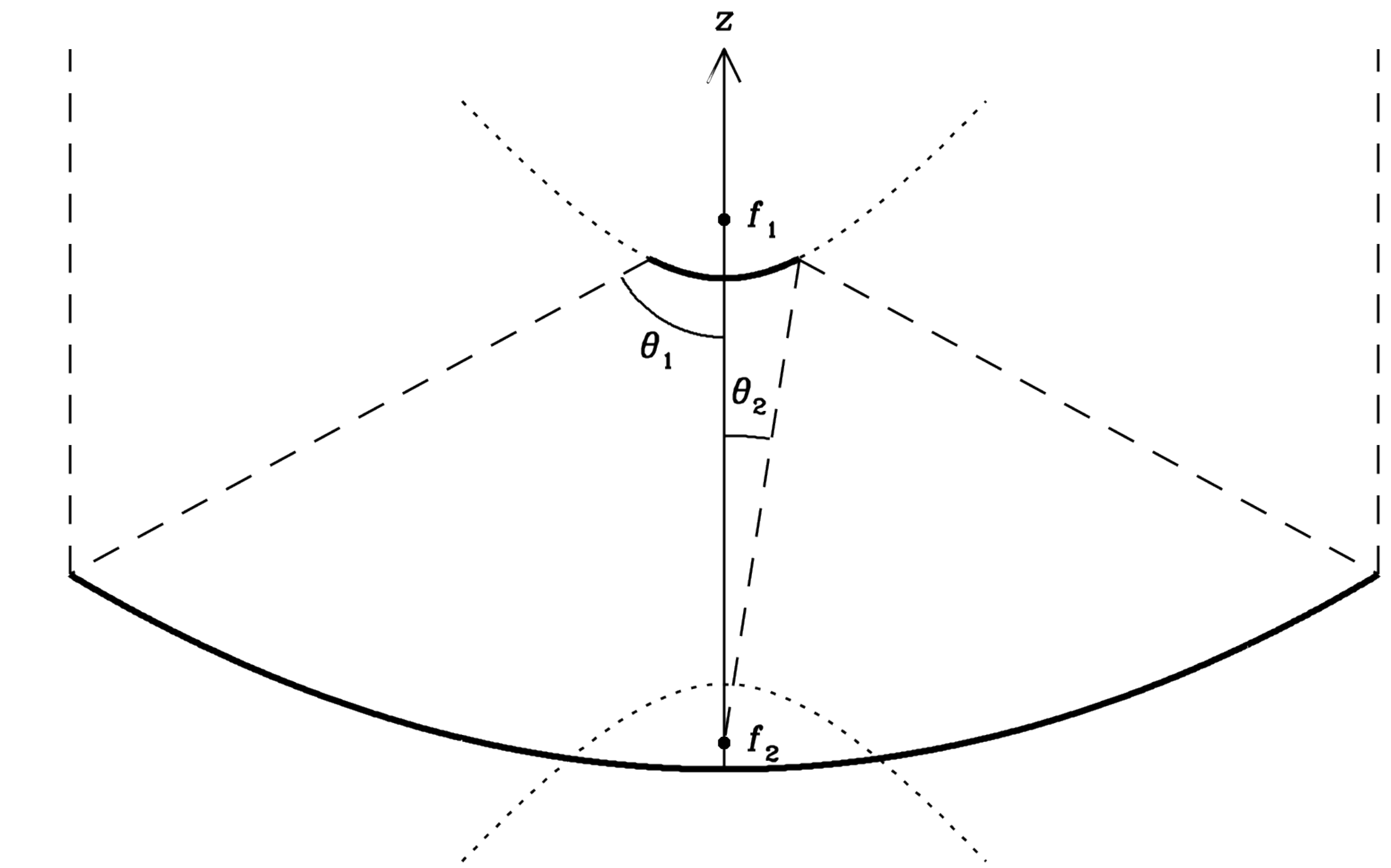
Radio telescopes are so large that paraboloids with high f/D ratios are impractical; typically  $f/D \approx 0.4$ . Thus radio “dishes” are relatively deep, as shown in the Figure.

A consequence of a low ratio is a **tiny field of view at the prime focus**. The instantaneous imaging capability of a large single dish is severely limited by the small number of feeds (detectors) that can fit into the tiny focal circle.

Cross section of a radio telescope rotationally symmetric around the z-axis (*and having a Cassegrain subreflector*).

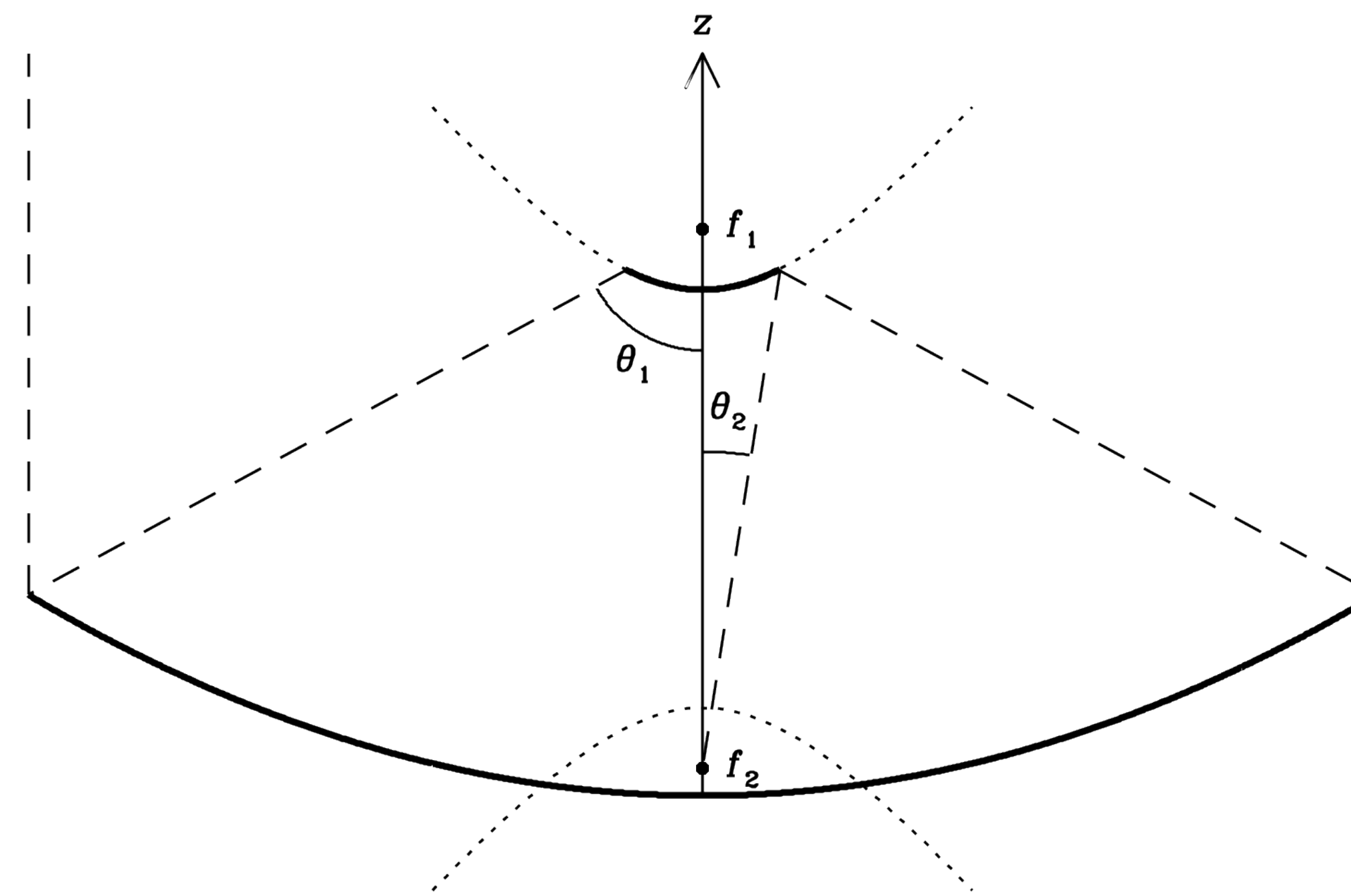
Parallel rays from a distant radio source are reflected by a circular paraboloid whose **prime focus** is at the point marked  $f_1$ .

The convex Cassegrain subreflector is a circular hyperboloid located below the prime focus. It reflects these rays to the feed located at the **secondary focus**  $f_2$  just above the vertex of the paraboloid.



# Radio telescopes

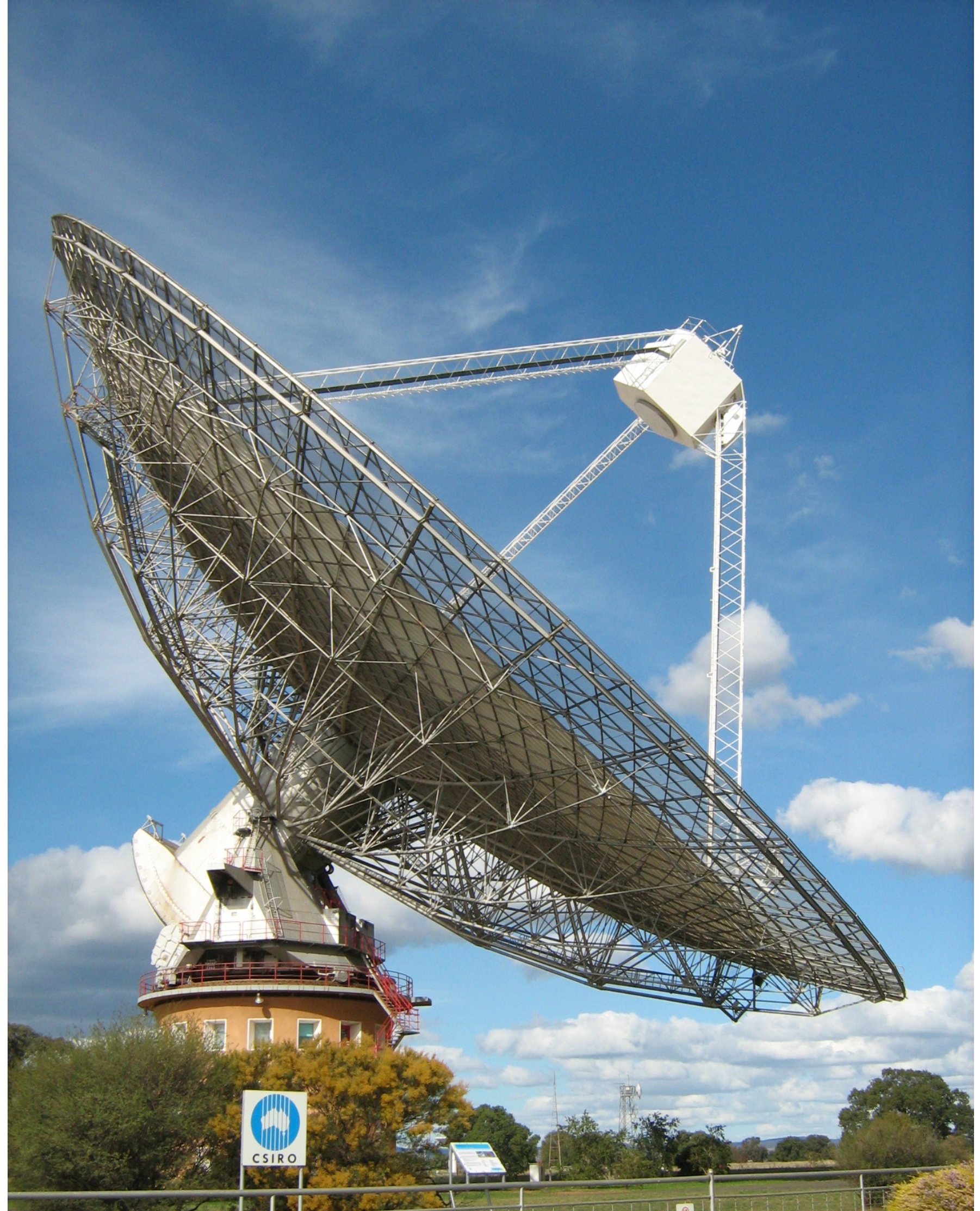
The Figure shows the optical system of the 140-foot telescope. Radiation reflected from the main dish is reflected a second time from the convex Cassegrain **subreflector** located just below the focal point down to feed horns and receivers near the vertex of the paraboloid.



The 140-foot (43-m) telescope in Green Bank

# Radio telescopes

The 60m Murriyang telescope had the detectors in the prime focus.



60m Murriyang in Parkes, Australia

# Radiometer

- A radio receiver used to measure the average power of the noise coming from a radio telescope in a well-defined frequency range is called a **radiometer**. The noise voltage has a Gaussian amplitude distribution with zero mean, and it fluctuates on the very short timescales (nanoseconds) comparable with the inverse of the radiometer bandwidth  $\Delta\nu$ .
- A **square-law detector** in the radiometer squares the input noise voltage to produce an output voltage proportional to the input noise power. Noise power is always greater than zero, and the noise from most astronomical sources is **stationary**, meaning that its mean power is steady when averaged over much longer timescales  $\tau$  (seconds to hours).
- By averaging a large number  $N=(2\Delta\nu\tau)$  of independent noise samples, an ideal radiometer can determine the average noise power with a fractional uncertainty as small as  $(N/2)^{-1/2} = (\Delta\nu\tau)^{-1/2} < 1$  and detect faint sources that increase the antenna temperature by only a tiny fraction of the total noise power. The ideal radiometer equation expresses this result in terms of the radiometer bandwidth and the averaging time.
- Gain variations in practical radiometers, fluctuations in atmospheric emission, and confusion by unresolved radio sources may significantly degrade the actual sensitivity compared with that predicted by the ideal radiometer equation.

# Radiometer

It is convenient to describe noise power in units of temperature. The noise power per unit bandwidth generated by a resistor of temperature  $T$  is  $P_\nu = kT$  in the low-frequency limit, so we can define the **noise temperature** of *any* noiselike source in terms of its power per unit bandwidth  $P_\nu$ , where  $k$  is the Boltzmann's constant.

$$T_N \equiv \frac{P_\nu}{k}$$

The temperature equivalent to the *total* noise power from all sources referenced to the input of a radiometer connected to the output of a radio telescope is called the **system noise temperature**  $T_s$ . It is the sum of many contributors to the antenna temperature plus the radiometer noise temperature  $T_r$

$$T_s = T_{\text{cmb}} + T_{\text{rsb}} + \Delta T_{\text{source}} + [1 - \exp(-\tau_A)] T_{\text{atm}} + T_{\text{spill}} + T_r + \dots$$

# Radiometer

$$T_s = T_{\text{cmb}} + T_{\text{rsb}} + \Delta T_{\text{source}} + [1 - \exp(-\tau_A)] T_{\text{atm}} + T_{\text{spill}} + T_r + \dots$$

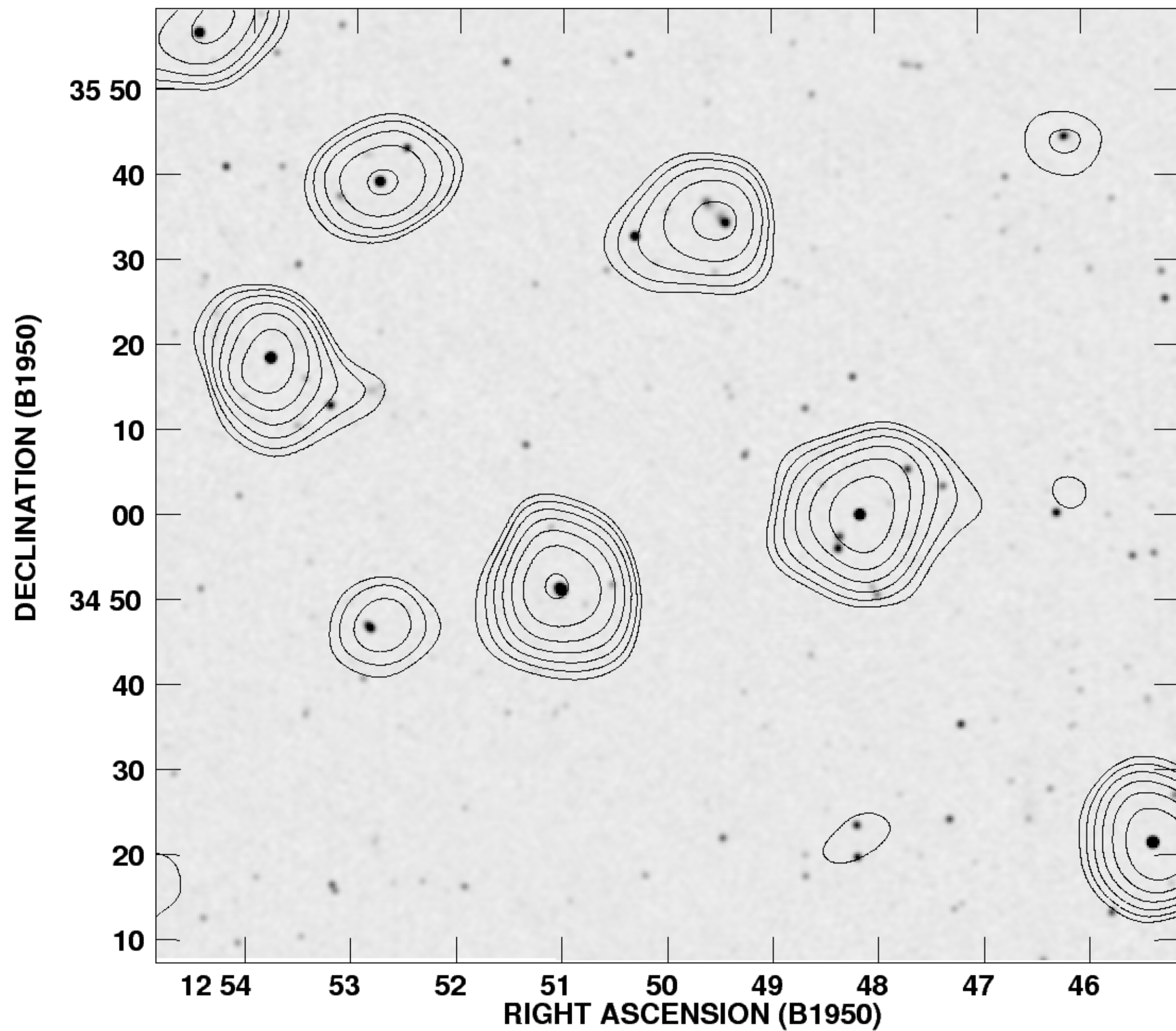
There are seven antenna-temperature contributions listed explicitly in Equation:

1.  $T_{\text{cmb}} = 3.5K$  is from the nearly isotropic cosmic microwave background.
2.  $T_{\text{rsb}}$  is the average sky brightness temperature contributed by all “background” radio sources.
3.  $\Delta T_{\text{source}}$  is from the astronomical source being observed, written with a  $\Delta$  to emphasize that it is usually much smaller than the total system noise:  $\Delta T_{\text{source}} < T_s$
4.  $[1 - \exp(-\tau_A)] T_{\text{atm}}$  is the brightness of atmospheric emission in the telescope beam
5.  $T_{\text{spill}}$  accounts for spillover radiation that the feed picks up in directions beyond the edge of the reflector, primarily from the ground.
6.  $T_r$  is the **radiometer noise temperature** attributable to noise generated by the radiometer itself. This can be minimised by cryogenically cooling the radiometer.
7. ... represents any other noise sources that might be important.

# Confusion

- Single-dish radio telescopes have large collecting areas but relatively broad beams at long wavelengths.
- Nearly all discrete continuum sources are extragalactic and extremely distant, so they are distributed randomly and isotropically on the sky.
- The sky-brightness fluctuations caused by numerous faint sources in every telescope beam are called **confusion**, and confusion usually limits the sensitivity of single-dish continuum observations at frequencies below  $\nu \sim 10$  GHz.
- The Figure shows contours from a portion of that low-resolution image superimposed on an overlapping high-resolution gray-scale image.

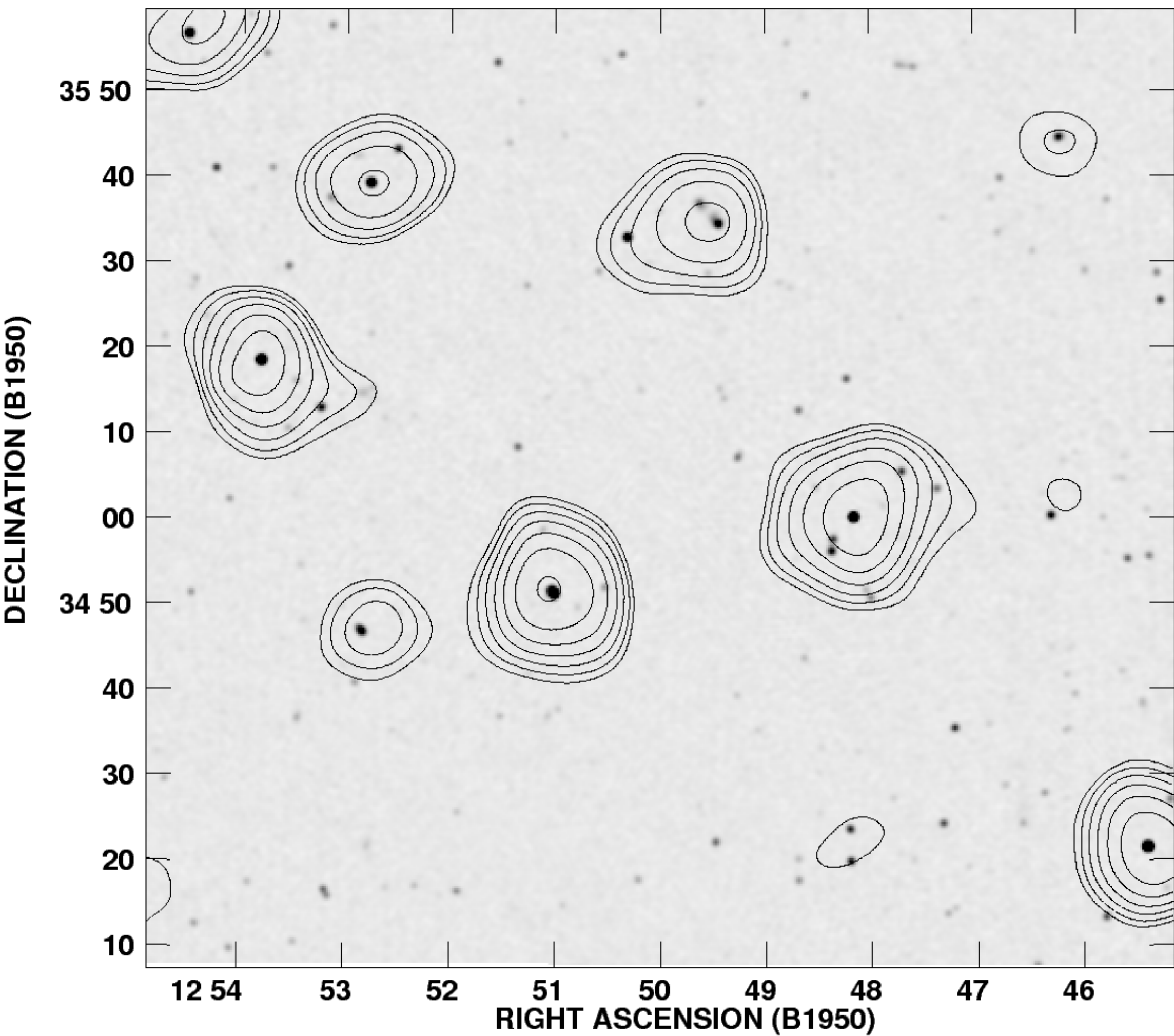
Contours: 300-foot telescope, image: VLA 1.4 GHz  
image at a substantially better resolution.



# Confusion

- Individual sources fainter than the **confusion limit**  $\approx 5\sigma_c$  cannot be detected reliably, no matter how low the receiver noise.
- Most continuum observations of faint sources at frequencies below  $\nu \sim 10$  GHz are made with interferometers instead of single dishes because interferometers can synthesize much smaller beamwidths  $\theta$  and hence have significantly lower confusion limits.
- Confusion by steady continuum sources has a much smaller effect on observations of spectral lines or rapidly varying sources such as pulsars.

Contours: 300-foot telescope, image: VLA 1.4 GHz  
image at a substantially better resolution.



# Single-dish telescopes



Effelsberg telescope



Green Bank telescope

**Every practical single-dish radio telescope has relatively low angular resolution and pointing accuracy, small field-of-view, and limited sensitivity.**

- The largest fully steerable dish has diameter  $D \sim 100\text{m}$  and its angular resolution is diffraction limited to  $\theta = \lambda/D$  radians, so impossibly large diameters would be needed to achieve sub-arcsecond resolution at radio wavelengths.
- **Pointing and source-tracking accuracy** is also a problem for a large single dish. The telescope beam should be able to follow a radio source on the sky within  $\sigma \sim \theta/10$  for reasonably accurate photometry or imaging.
- Gravitational sagging, **telescope deformations** caused by differential solar heating, and torques caused by wind gusts combine to limit the mechanical tracking and pointing accuracies of the best radio telescopes to  $\sigma \sim 1 \text{ arcsec}$ .
- Most optical telescopes can make high-resolution images covering large areas of sky rapidly because their large fields-of-view  $\Omega_{FOV} > \theta^2$  cover millions or billions of pixels.
- In contrast, most single-dish radio telescopes have only one or several beams.
- The **geometric area** of a single dish is just  $\pi D^2/4$  while the geometric area  $N\pi D^2/4$  of an interferometer with  $N$  dishes can be arbitrarily large.
- The *continuum* sensitivity of a single dish is strongly limited by **confusion** at frequencies below about 10 GHz.

# Interferometers



Aperture-synthesis interferometers comprising  $N \geq 2$  moderately small dishes have mitigated these and many other practical problems associated with single dishes, such as vulnerability to fluctuations in atmospheric emission and receiver gain, radio-frequency interference, and pointing shifts caused by atmospheric refraction.

For example, the **Westerbork Synthesis Radio Telescope (WSRT)** consists of  $N=14$ ,  $D=25\text{m}$  telescopes on east–west baselines up to  $b \approx 3\text{km}$  in length.

Its total collecting area is that of a single dish with diameter  $D_{tot} = N^{1/2}D = 92\text{ m}$ .

It has the high angular resolution of a diffraction-limited telescope 3 km in diameter.

It has the large instantaneous field-of-view of a 25-m telescope, so it can image  $\sim (b/D)^2 \sim 10^4$  pixels at once with only one receiver on each telescope.

It can measure positions of radio sources with subarcsecond accuracy despite the much larger source-tracking errors of the individual telescopes.

# Interferometers



ALMA



JVLA

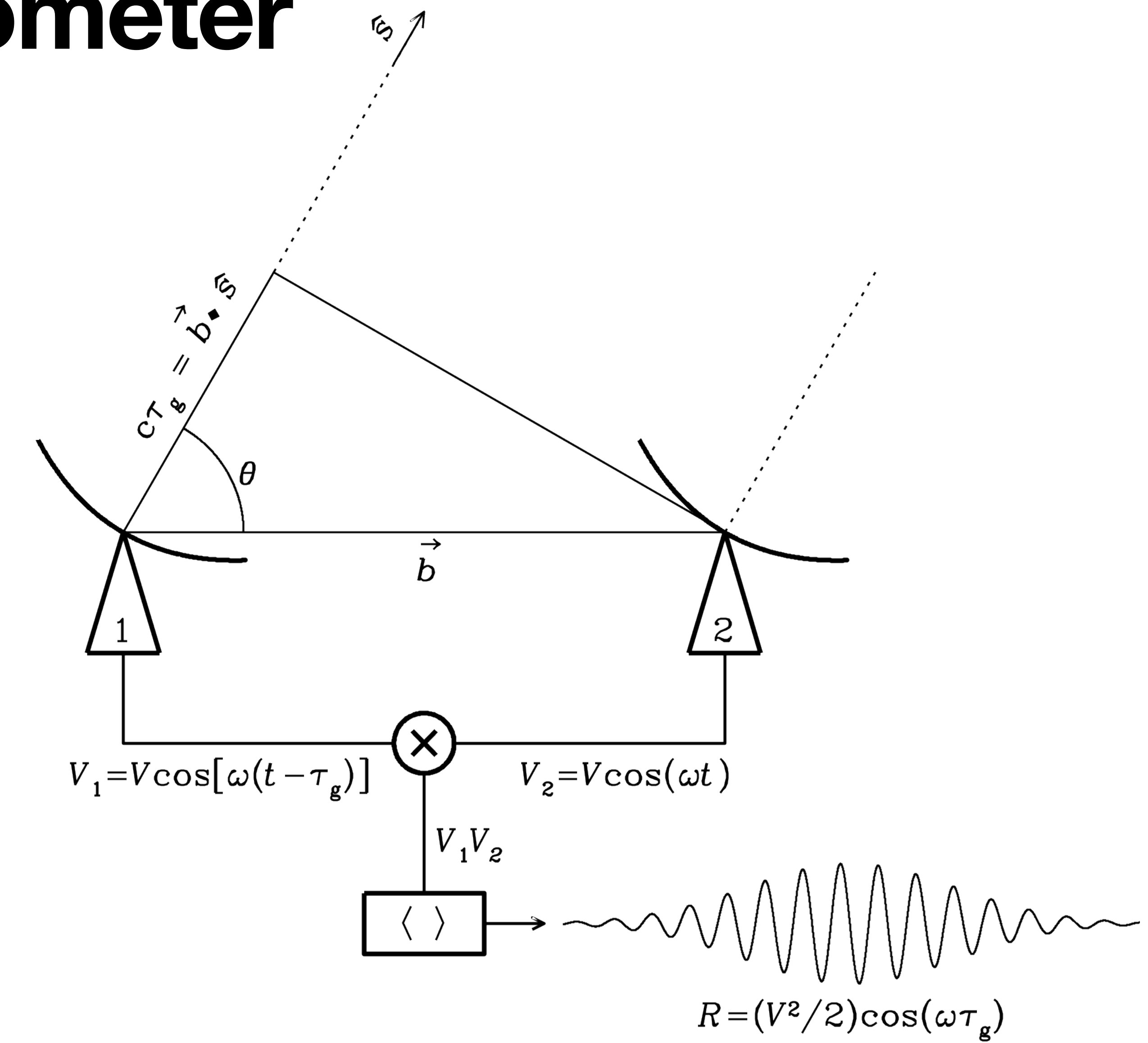
Historically, the total bandwidths and numbers of simultaneous frequency channels of aperture-synthesis interferometers with many dishes were lower than those of single dishes. -> **intense computational need**. Recent advances in correlator electronics and computing have largely overcome these practical limitations, so new or updated interferometers such as ALMA (The Atacama Large Millimetre Array) and the JVLA (Karl G. Jansky Very Large Array) are playing an increasingly dominant role in observational radio astronomy.

The **primary uses of single dishes** today are

- observing **pulsars**, which are time variable so they are easy to separate from confusion by time-independent continuum sources;
- spectroscopic observations of **extended low-brightness sources**, again largely immune to confusion;
- complementing interferometers by providing “**zero-spacing**” data on very extended sources or by serving as elements of very long baseline arrays.

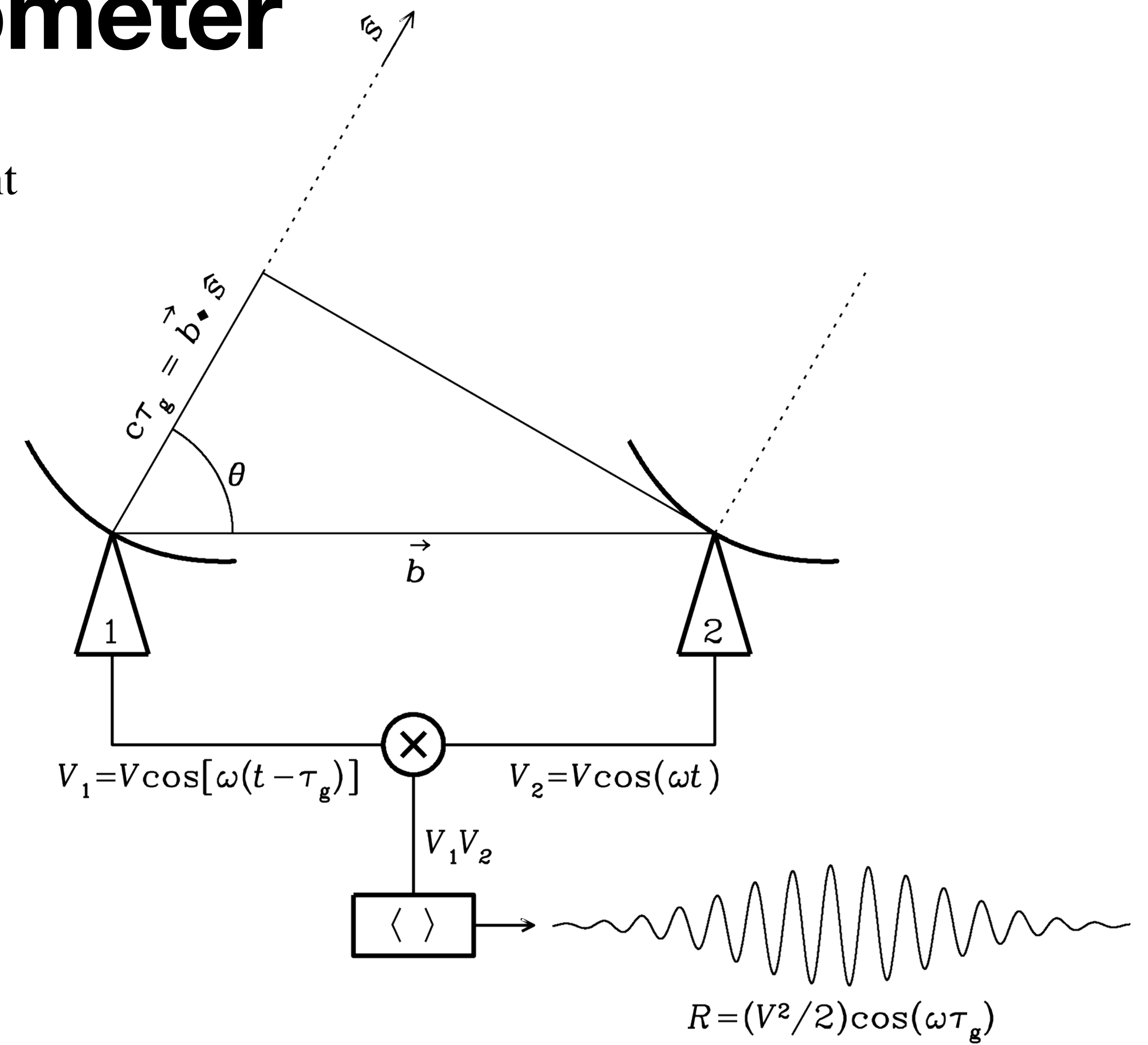
# Two element interferometer

- The simplest radio **interferometer** is a pair of radio telescopes whose voltage outputs are **correlated** (multiplied and averaged),
- and even the most elaborate interferometers with  $N \gg 2$  antennas, often called **elements**, can be treated as  $N(N-1)/2$  independent two-element interferometers.



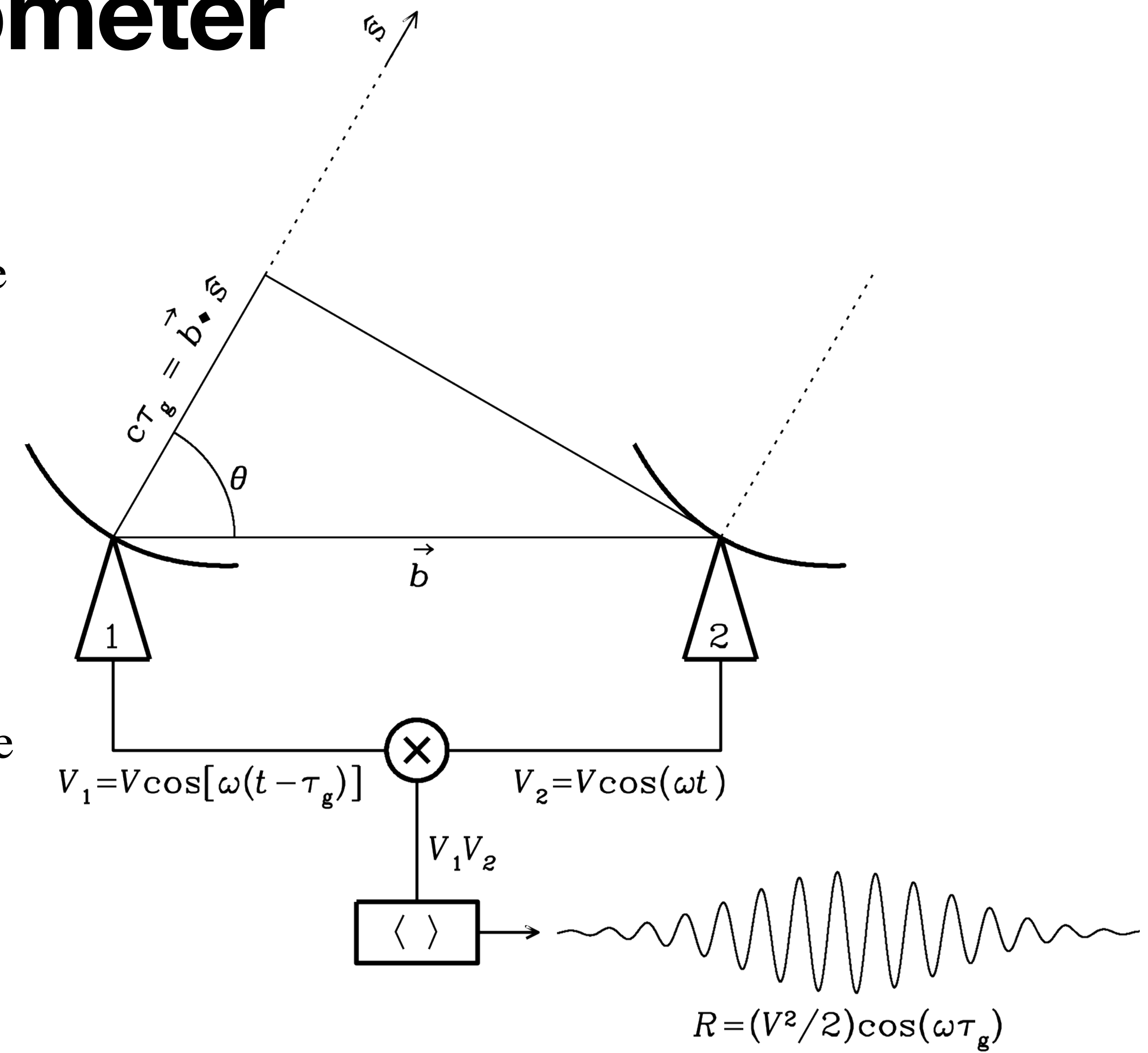
# Two element interferometer

- This diagram shows the components of a two-element quasi-monochromatic multiplying interferometer observing in a very narrow radio frequency range centered on  $\nu=\omega/(2\pi)$ .
- $\hat{s}$  is the unit vector in the direction of a distant point source and
- $\vec{b}$  is the baseline vector pointing from antenna 1 to antenna 2.
- The output voltage  $V_1$  of antenna 1 is the same as the output voltage  $V_2$  of antenna 2, but it is retarded by the **geometric delay**  $\tau_g = \vec{b} \cdot \hat{s} / c$  representing the **additional light-travel delay to antenna 1** for a plane wavefront from a source at angle  $\theta$  from the baseline vector.



# Two element interferometer

- These voltages are amplified, multiplied ( $\times$ ), and time averaged ( $\langle \rangle$ ) by the correlator to yield an **output response** whose amplitude  $R$  is **proportional to the flux density of the point source** and whose phase ( $\omega\tau_g$ ) depends on the delay and the frequency.
- The quasi-sinusoidal **output fringe** shown occurs if the source direction in the interferometer frame is changing at a constant rate  $d\theta/dt$ .
- The broad **Gaussian envelope** of the fringe shows the primary-beam attenuation as the **source passes through the beam** of the dishes.



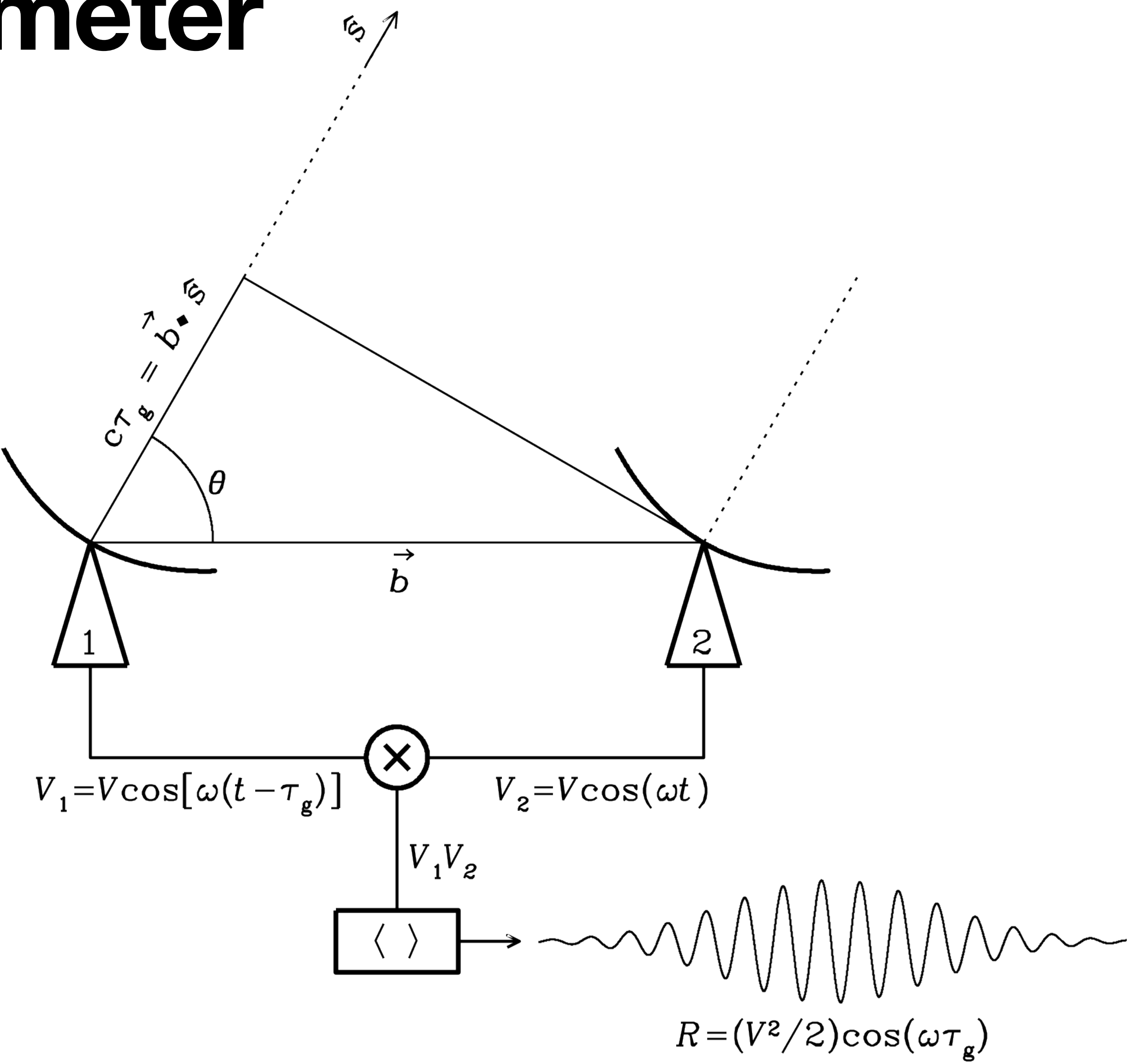
# Two element interferometer

- The correlator output voltage  $R=(V^2/2)\cos(\omega\tau_g)$  varies sinusoidally as the Earth's rotation changes the source direction relative to the baseline vector. These sinusoids are **called fringes**, and the fringe phase

$$\phi = \omega\tau_g = \frac{\omega}{c} b \cos \theta$$

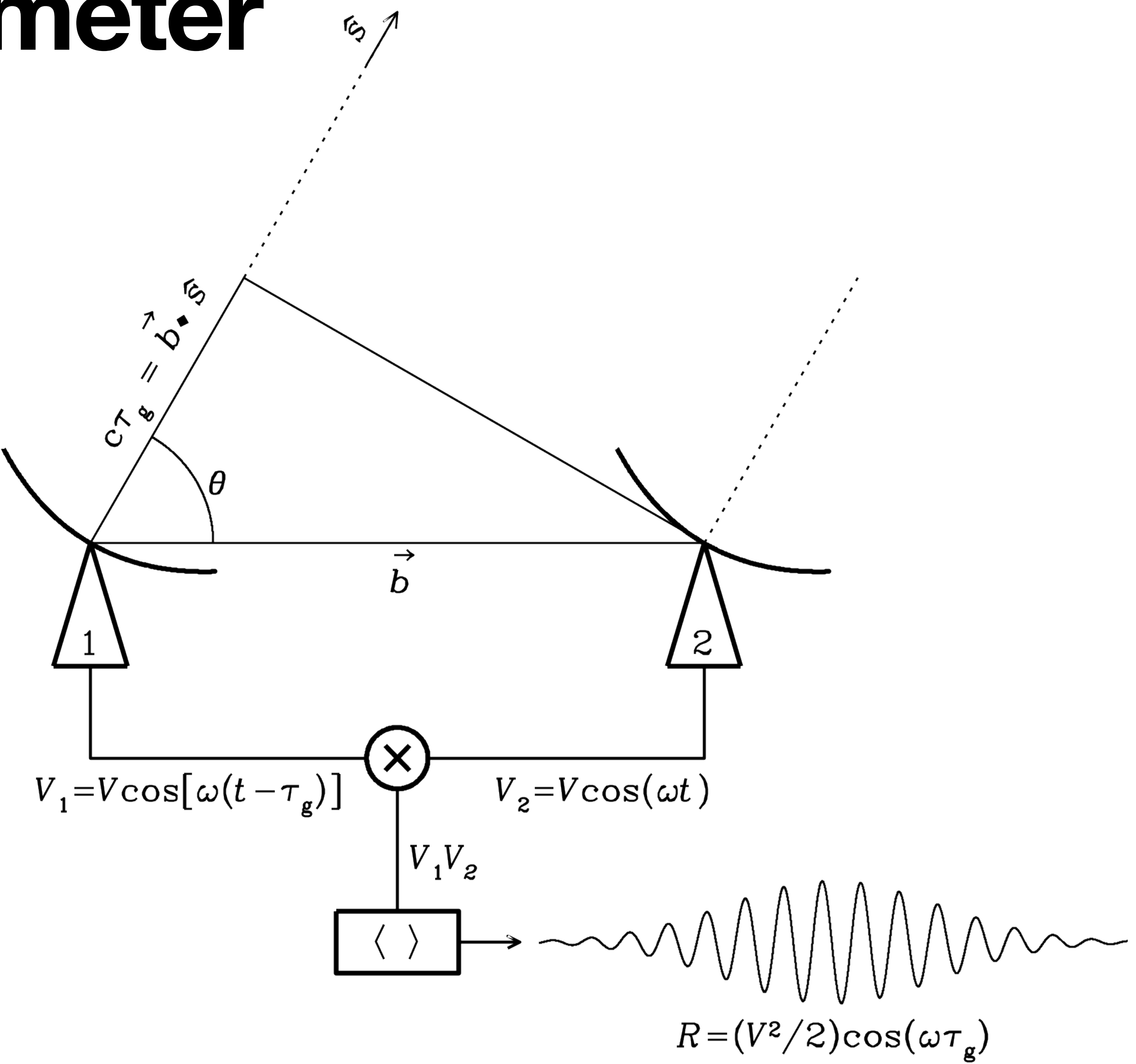
depends on  $\theta$  as follows:

$$\begin{aligned} \frac{d\phi}{d\theta} &= -\frac{\omega}{c} b \sin \theta \\ &= -2\pi \left( \frac{b \sin \theta}{\lambda} \right) \end{aligned}$$



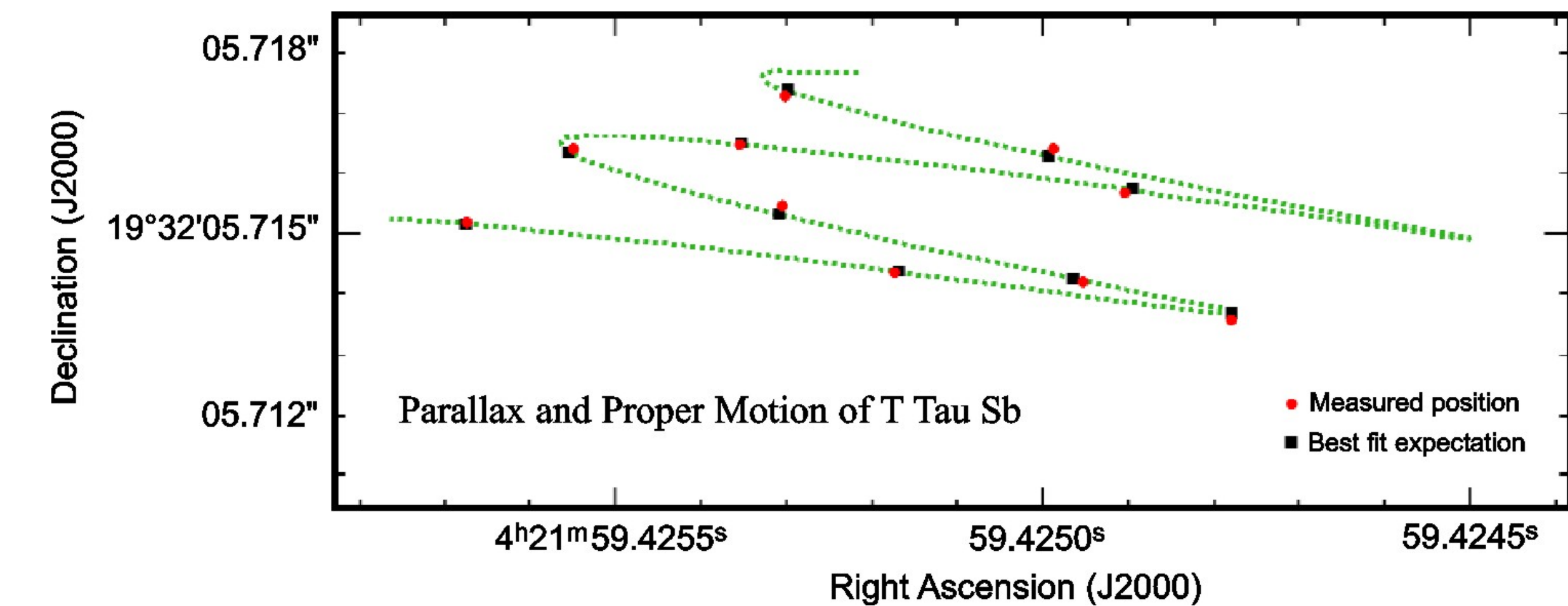
# Two element interferometer

- The fringe period  $\Delta\varphi=2\pi$  corresponds to an angular shift  $\Delta\theta=\lambda/(b\sin\theta)$ .
- The fringe phase is a sensitive measure of source position if the projected baseline  $b\sin\theta$  is many wavelengths long.
- Note that **fringe phase** and hence measured source position is not affected by small tracking errors of the individual telescopes. It **depends on time**, and times can be measured by clocks with much higher accuracy than angles (ratios of lengths of moving telescope parts) can be measured by rulers.
- An interferometer whose baseline is horizontal is not affected by the plane-parallel component of atmospheric refraction, which delays the signals reaching both telescopes equally.



# Two element interferometer

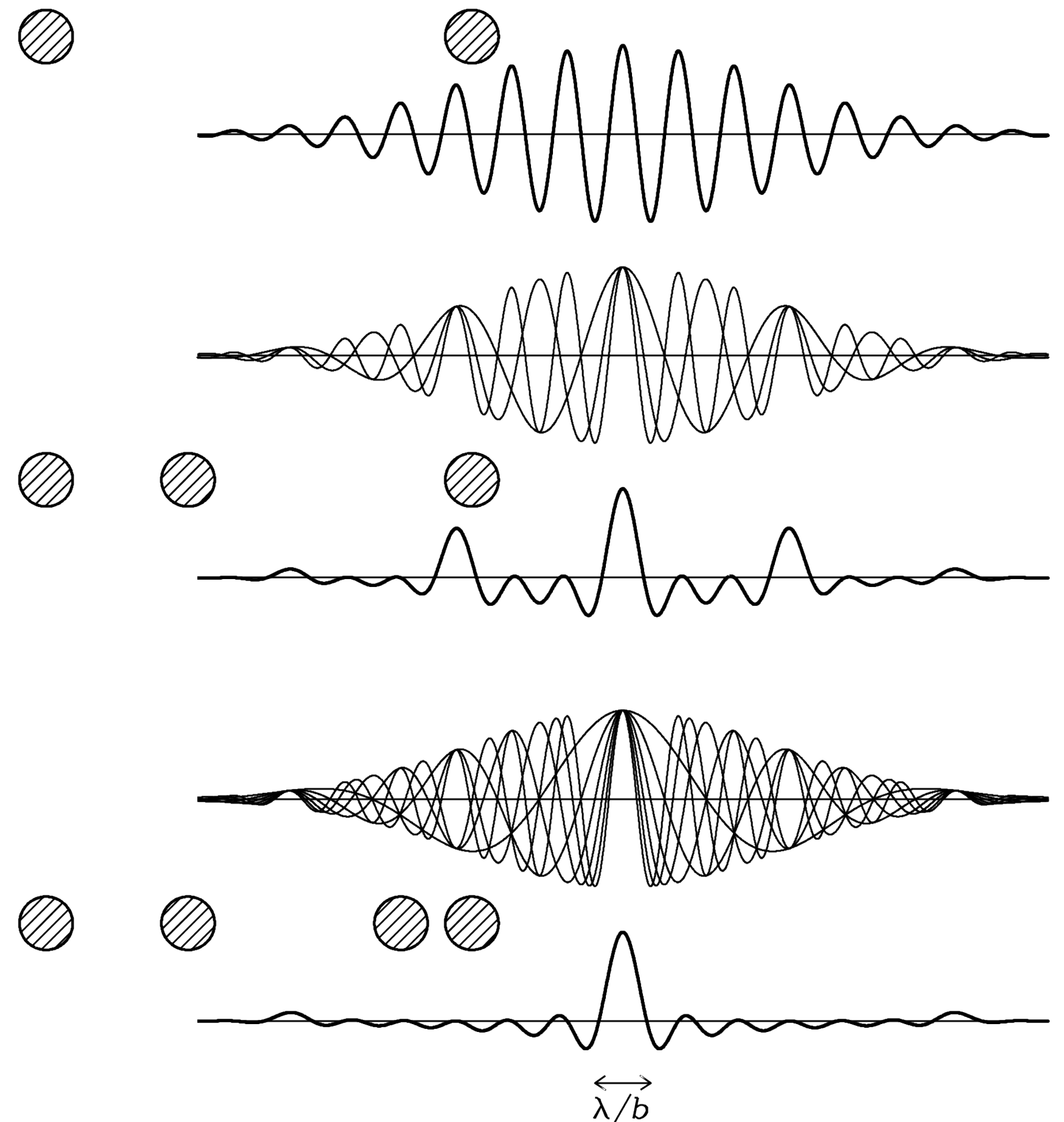
- Consequently, interferometers can determine the **positions of compact radio sources with unmatched accuracy**, as shown in Figure 1.6. Absolute positions with errors as small as  $\sigma\theta \approx 10^{-3}$  arcsec
- and differential positions with errors down to  $\sigma\theta \approx 10^{-5}$  arcsec  $< 10^{-10}$  rad have frequently been measured.



Multiepoch VLBA position measurements of T Tau Sb, young stellar object, allowed to determine its parallax distance with unprecedented accuracy:  $d=146.7 \pm 0.6$  pc, and even to **detect accelerated proper motion**.

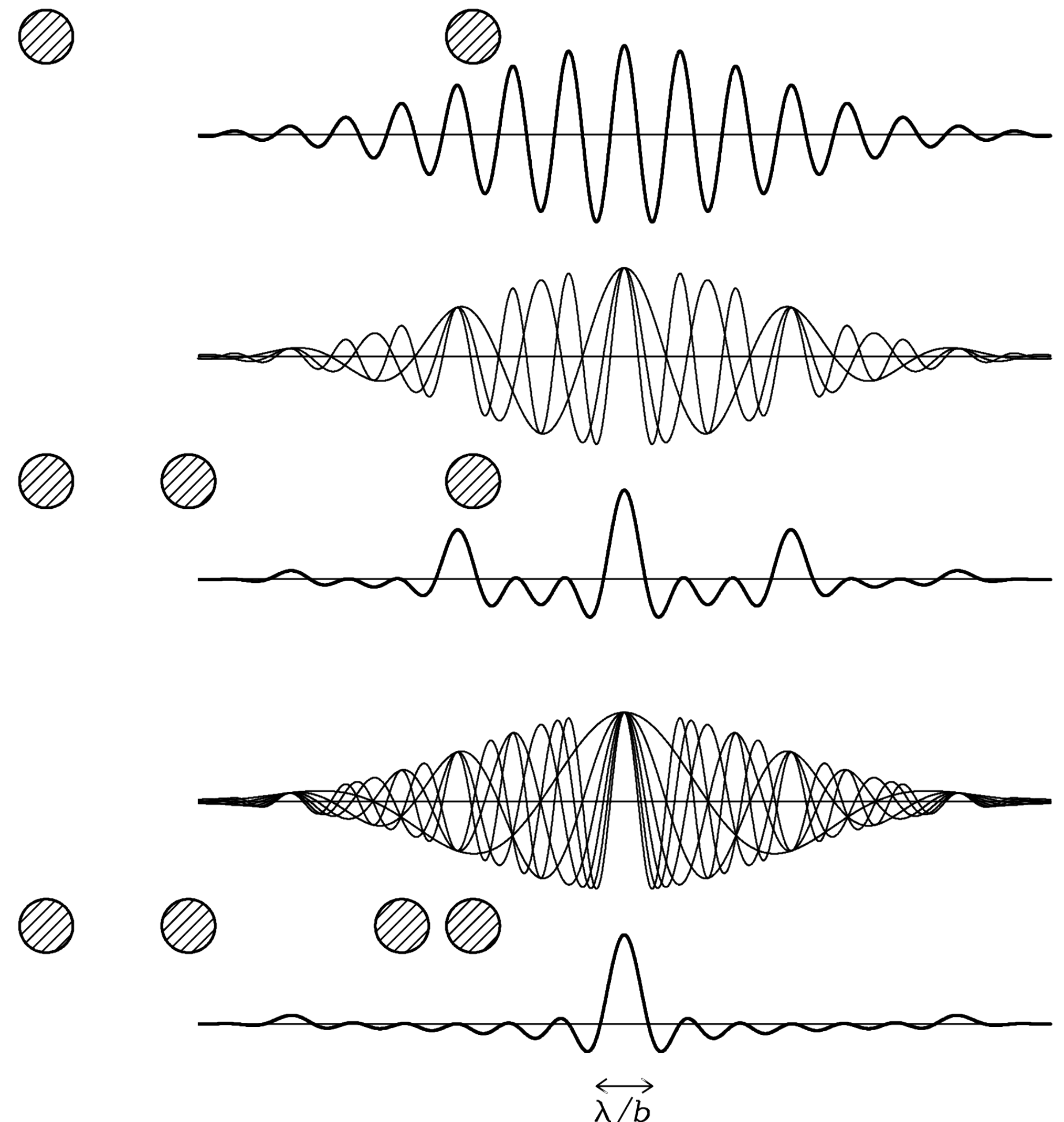
# Two element interferometer

- If the individual antennas comprising an interferometer were isotropic, the interferometer point-source response would be a sinusoid spanning the sky. Such an interferometer is sensitive to only one **Fourier component of the sky brightness distribution**: the component with angular period  $\lambda/(b\sin\theta)$ .
- The response  $R$  of a two-element interferometer with directive antennas is that sinusoid multiplied by the product of the voltage patterns of the individual antennas.
- Normally the two antennas are identical, so **this product is the power pattern of the individual antennas** and is called the **primary beam of the interferometer**.



# Two element interferometer

- The primary beam is usually a Gaussian much wider than a fringe period, as indicated in the Figure.
- The convolution theorem states that the Fourier transform of the product of two functions is the convolution of their Fourier transforms, so the interferometer with directive antennas **responds to a finite range of angular frequencies** centered on  $(b\sin\theta/\lambda)$ .
- Because the antenna diameters D must be smaller than the baseline b (else the antennas would overlap), **the angular frequency response cannot extend to zero** and the interferometer cannot detect an isotropic source—the bulk of the 3 K cosmic microwave background for example.
- The missing **short spacings** ( $b < D$ ) can be provided by a single-dish telescope with diameter  $D > b$ .
  - *Thus the  $D = 100 \text{ m}$  GBT can fill in the missing baselines  $b < 25\text{m}$  that the  $D = 25 \text{ m}$  VLA dishes cannot obtain.*



# Two element interferometer



+



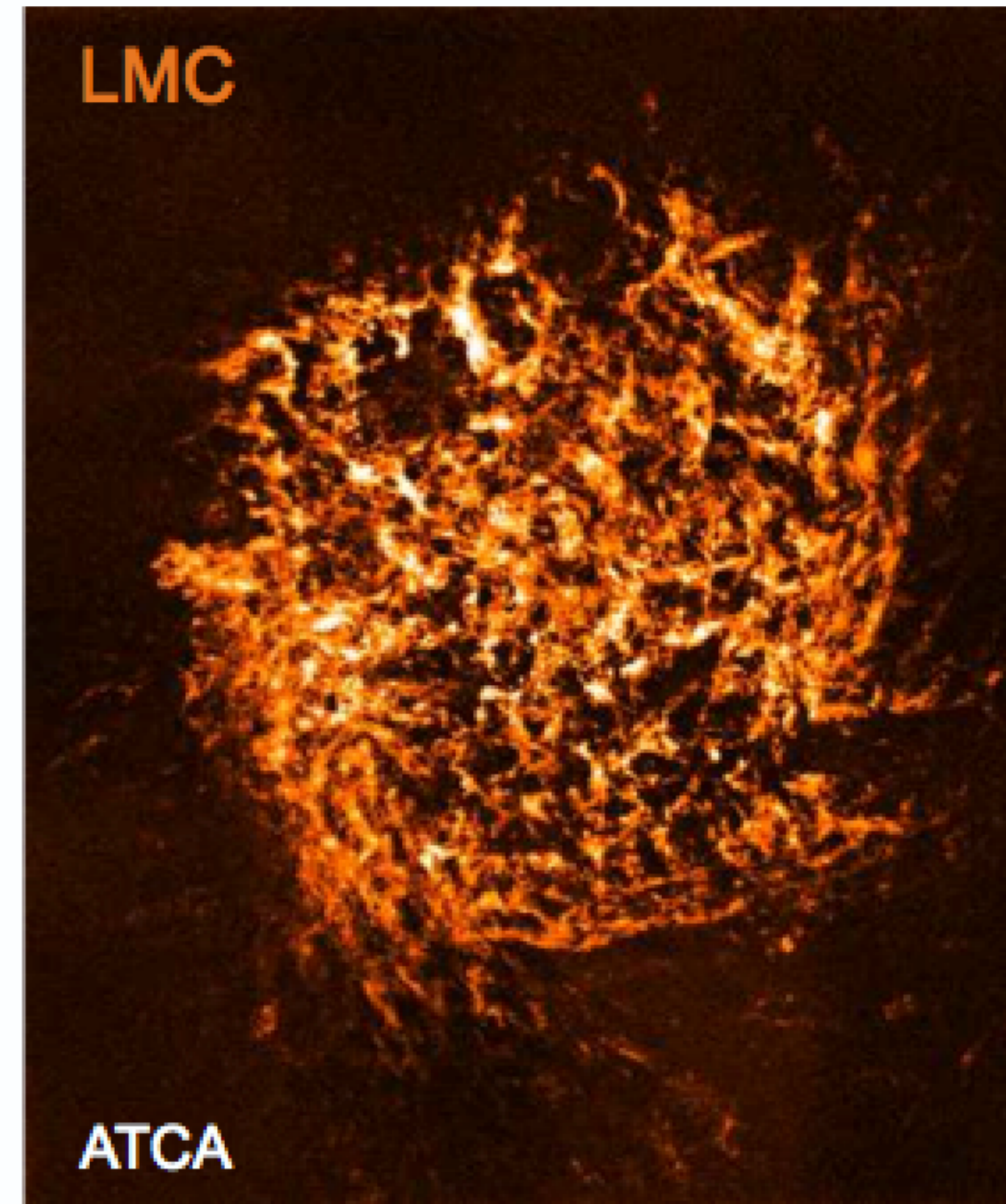
Single-dish for short spacing  
-> large angular scales

Interferometer for longer spacing  
-> small angular scales

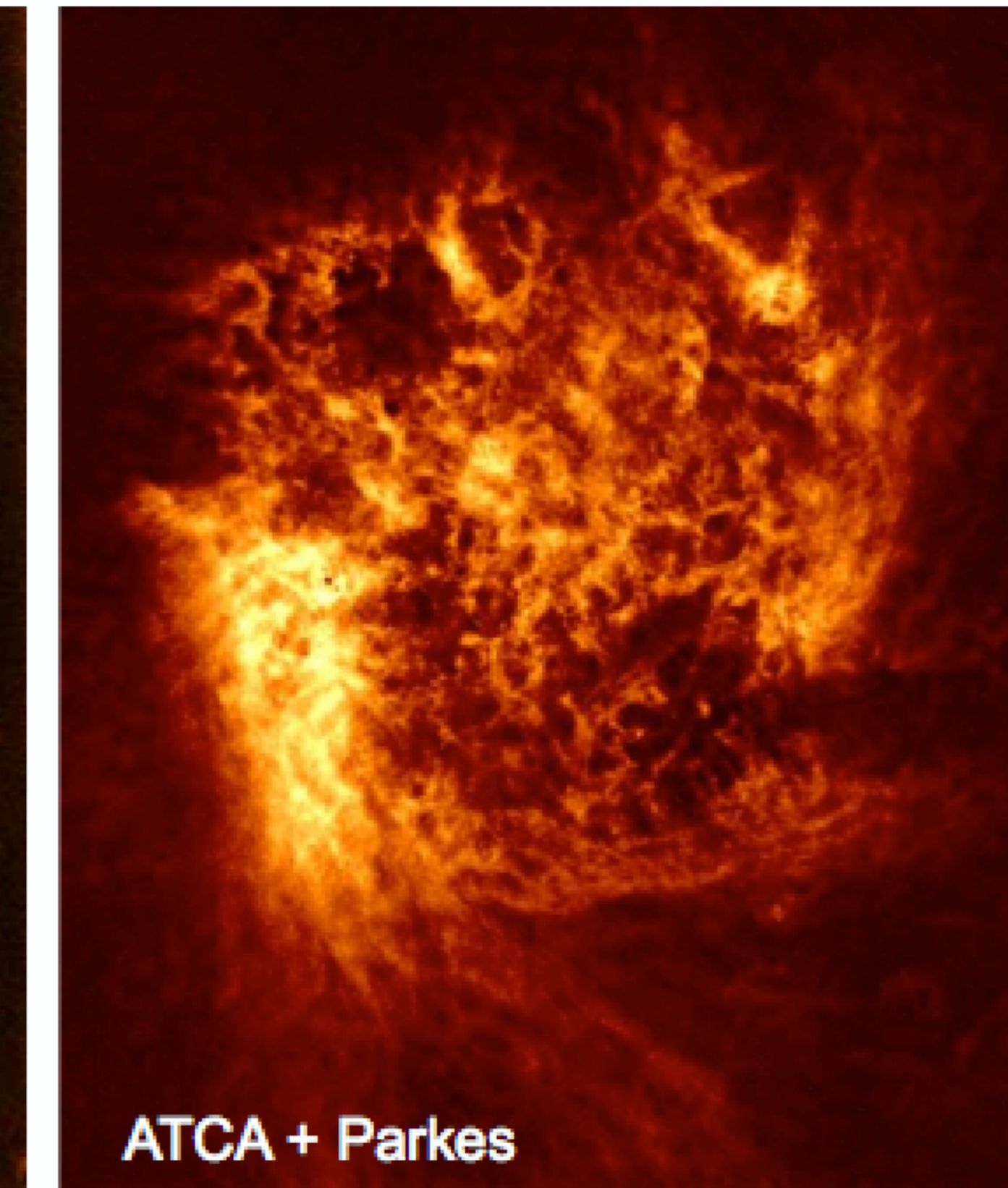
# Two element interferometer

Combining single dish  
and interferometer data

Interferometer only



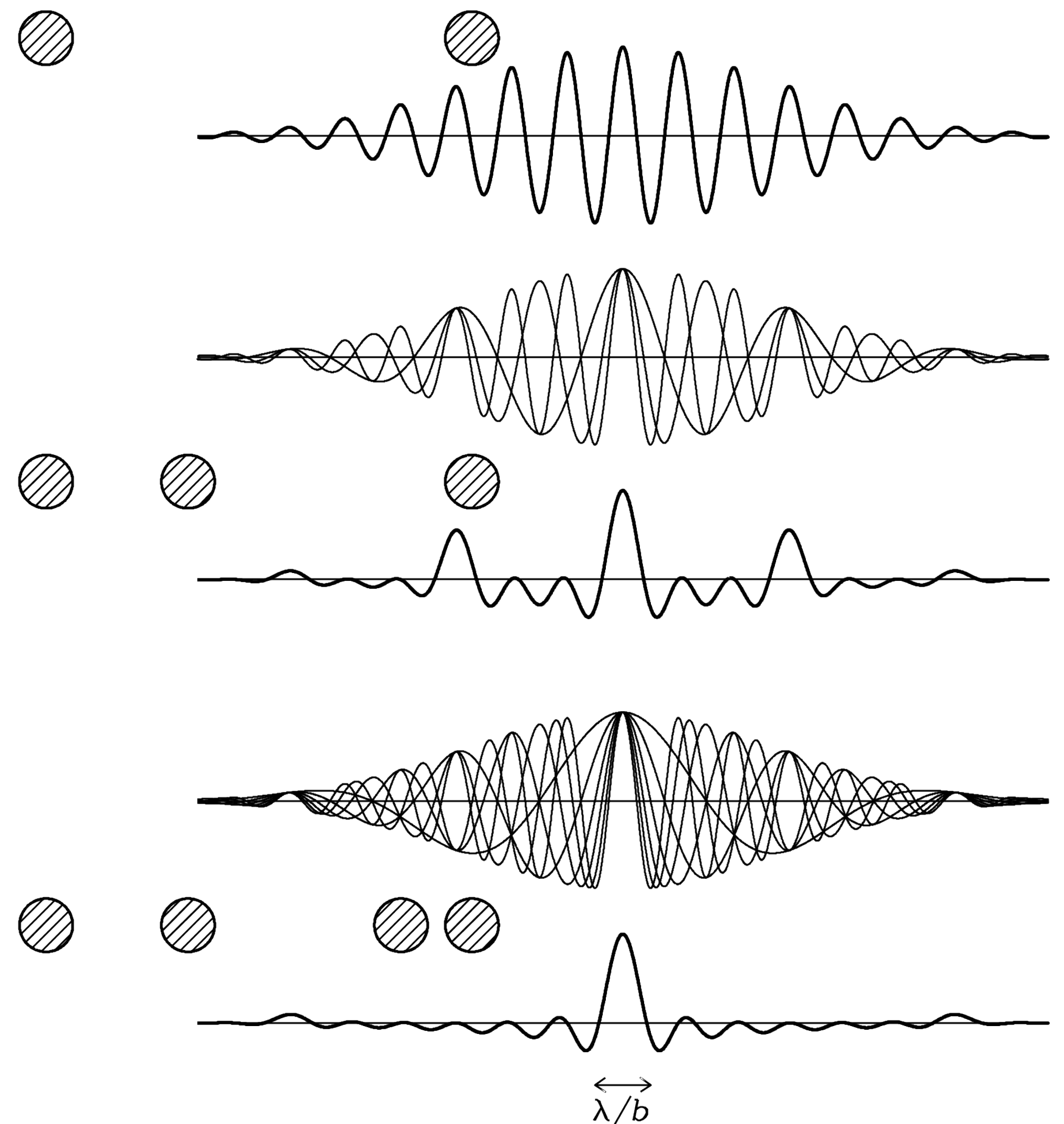
Interferometer + single dish



HI mosaic (1344 pointings) of the Large Magellanic Cloud by Kim et al. (1998, 2003).

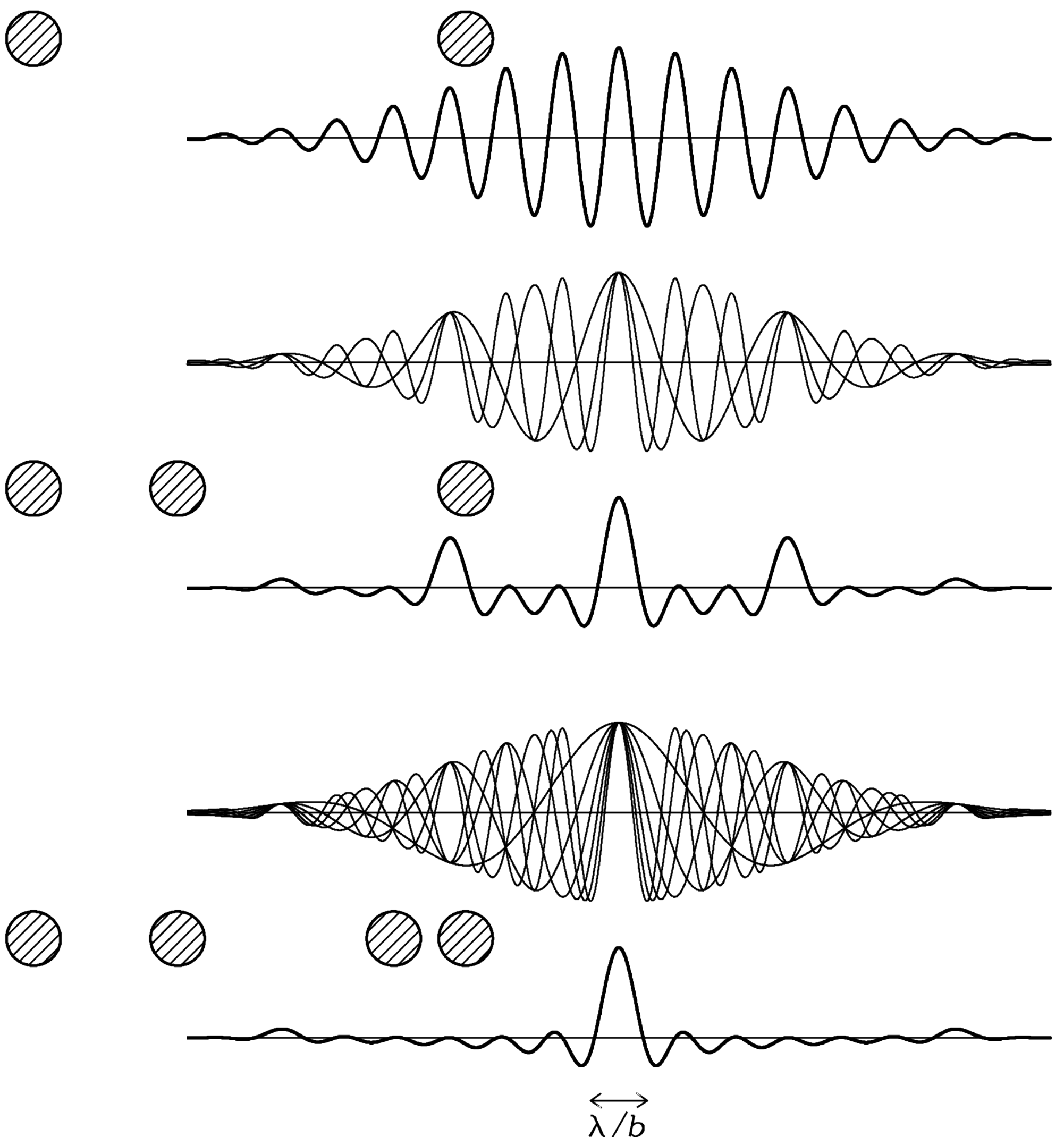
# Two element interferometer

- Improving the instantaneous point-source response pattern of an interferometer requires more Fourier components; that is, more baselines.
- An **interferometer with  $N$  antennas contains  $N(N-1)/2$  pairs of antennas**, each of which is a two-element interferometer, so the **instantaneous synthesized beam (the point-source response obtained by averaging the outputs of all of the two-element interferometers)** rapidly approaches a Gaussian as  $N$  increases.
- *The instantaneous point-source responses of a two-element interferometer with projected baseline length  $b$ , a three-element interferometer with three baselines (projected lengths  $b/3, 2b/3$ , and  $b$ ), and a four-element interferometer with six baselines (projected lengths  $b/6, 2b/6, 3b/6, 4b/6, 5b/6$ , and  $b$ ) are shown in the Figure.*



# Two element interferometer

- The instantaneous point-source responses of interferometers with overall projected length  $b$  and two, three, or four antennas distributed as shown are indicated by the thick curves.
- The **synthesized main beam** of the four-element interferometer is nearly Gaussian with angular resolution  $\theta \approx \lambda/b$ , but the **sidelobes** are still significant and there is a broad negative “bowl” caused by the lack of spacings shorter than the diameter of an individual antenna.
- Thus the **synthesized beam is sometimes called the dirty beam**. The instantaneous dirty beam of the multielement interferometer is the arithmetic mean of the individual responses of its component two-element interferometers.
- The individual responses of the three two-element interferometers comprising the three-element interferometer and of the six two-element interferometers comprising the four-element interferometer are plotted as thin curves.



# Two element interferometer

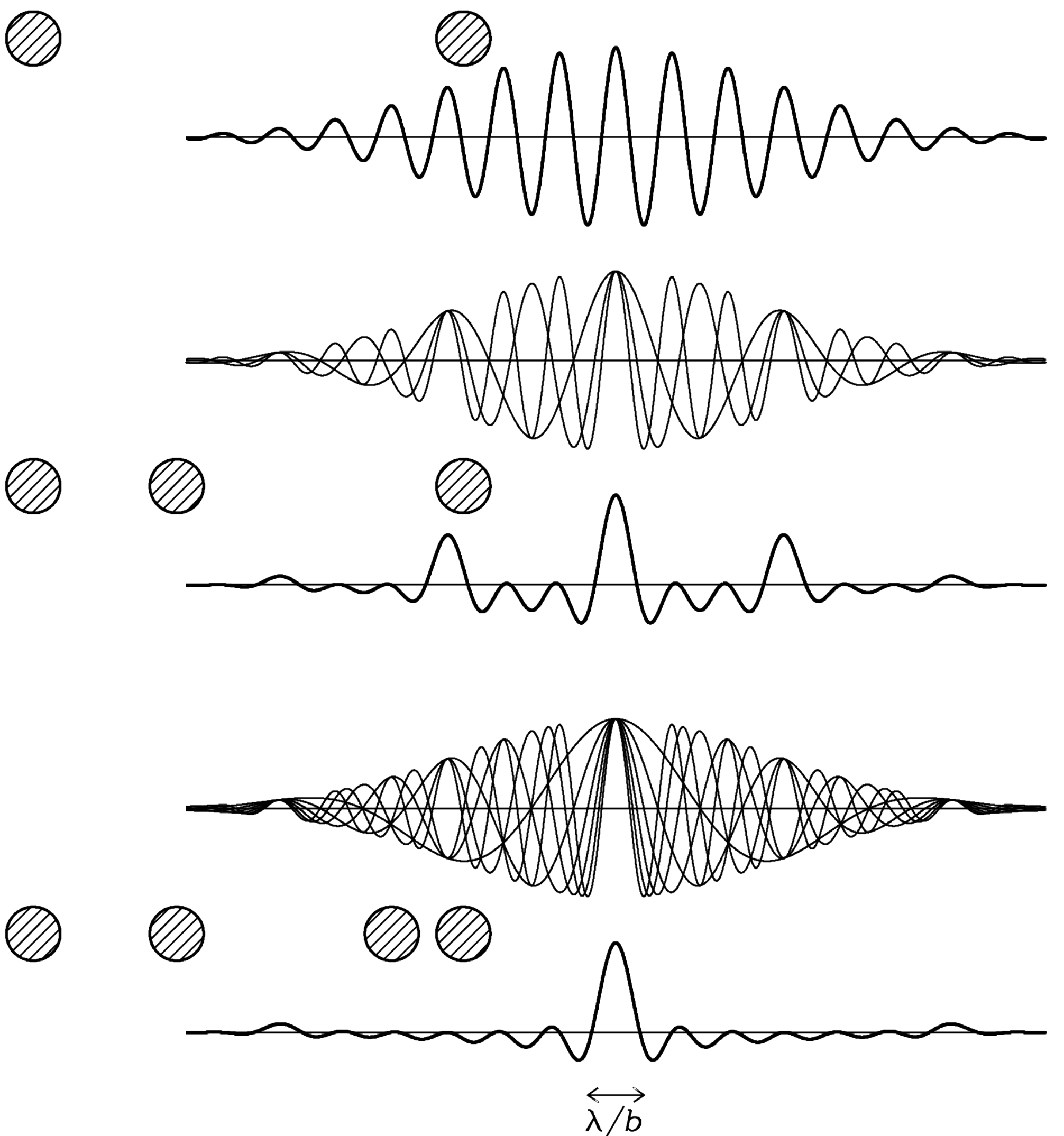
- Most radio sources are stationary; that is, their brightness distributions do not change significantly on the timescales of astronomical observations.
- **For stationary sources, a two-element interferometer with movable antennas could make  $N(N-1)/2$  observations to duplicate one observation with an  $N$ -element interferometer -> the observations do not need to happen at the same time.**
- Examples for movable interferometers: ALMA, JVLA, the Australia Telescope Compact Array (ATCA)



ATCA



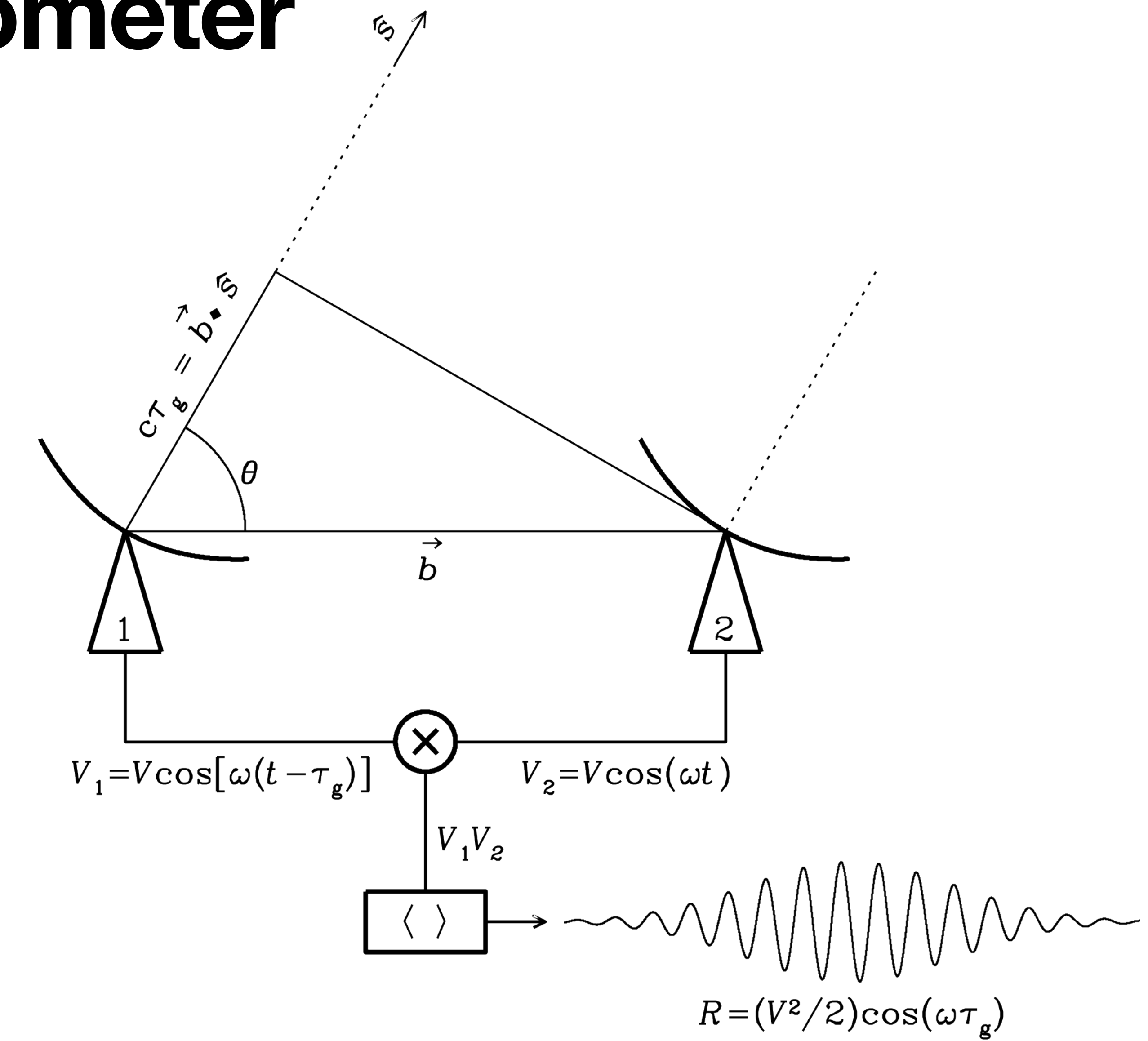
JVLA



# Two element interferometer

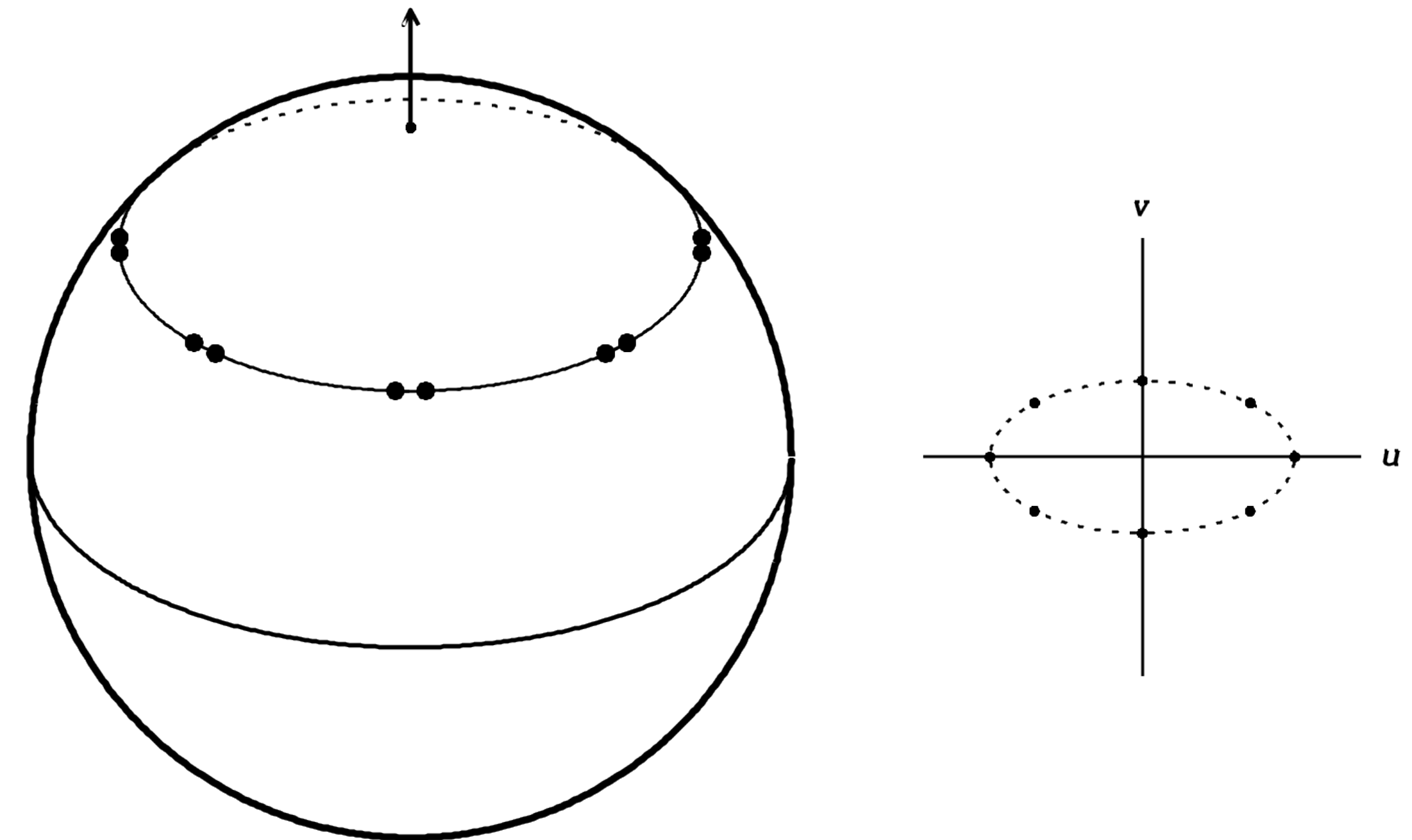
- The response to an extended source with brightness distribution  $I(\hat{s})$  of the two-element quasi-monochromatic interferometer with a complex correlator is the **complex visibility**

$$\mathcal{V} = \int I(\hat{s}) \exp(-i2\pi \vec{b} \cdot \hat{s}/\lambda) d\Omega.$$



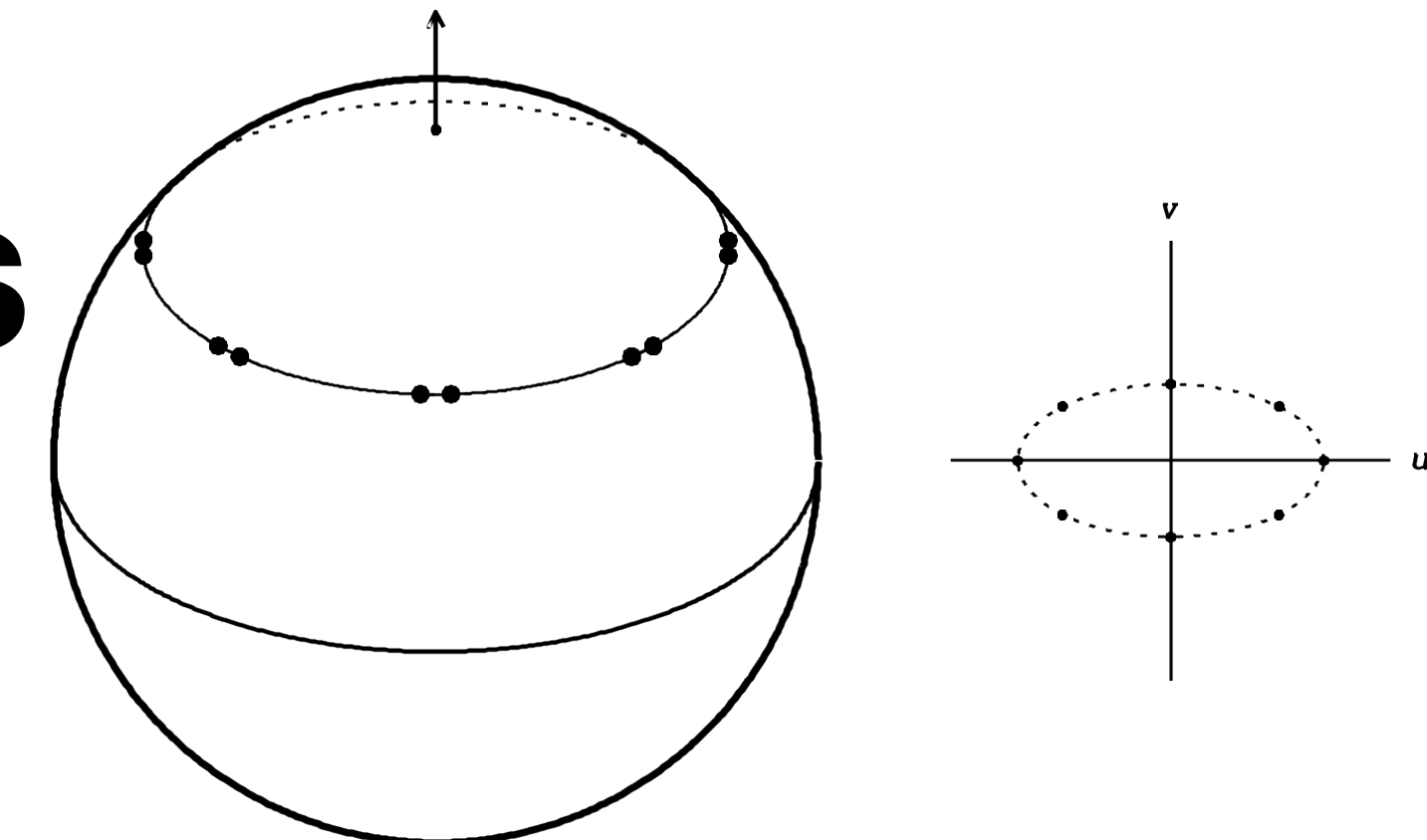
# Earth rotation aperture synthesis

- The Earth's rotation varies the projected baseline coverage of an interferometer whose elements are fixed on the ground.
- In particular, all baselines of an interferometer whose baselines are confined to an east–west line will remain in a single plane perpendicular to the Earth's north–south rotation axis as the Earth turns daily.
- Confining all baselines to two dimensions has the computational advantage that the **brightness distribution of a source is simply the two-dimensional Fourier transform of the measured visibilities**.
- The Figure illustrates Earth-rotation aperture synthesis by an east–west two-element interferometer at latitude  $+40^\circ$  as viewed from a source at declination  $\delta=+30^\circ$ .

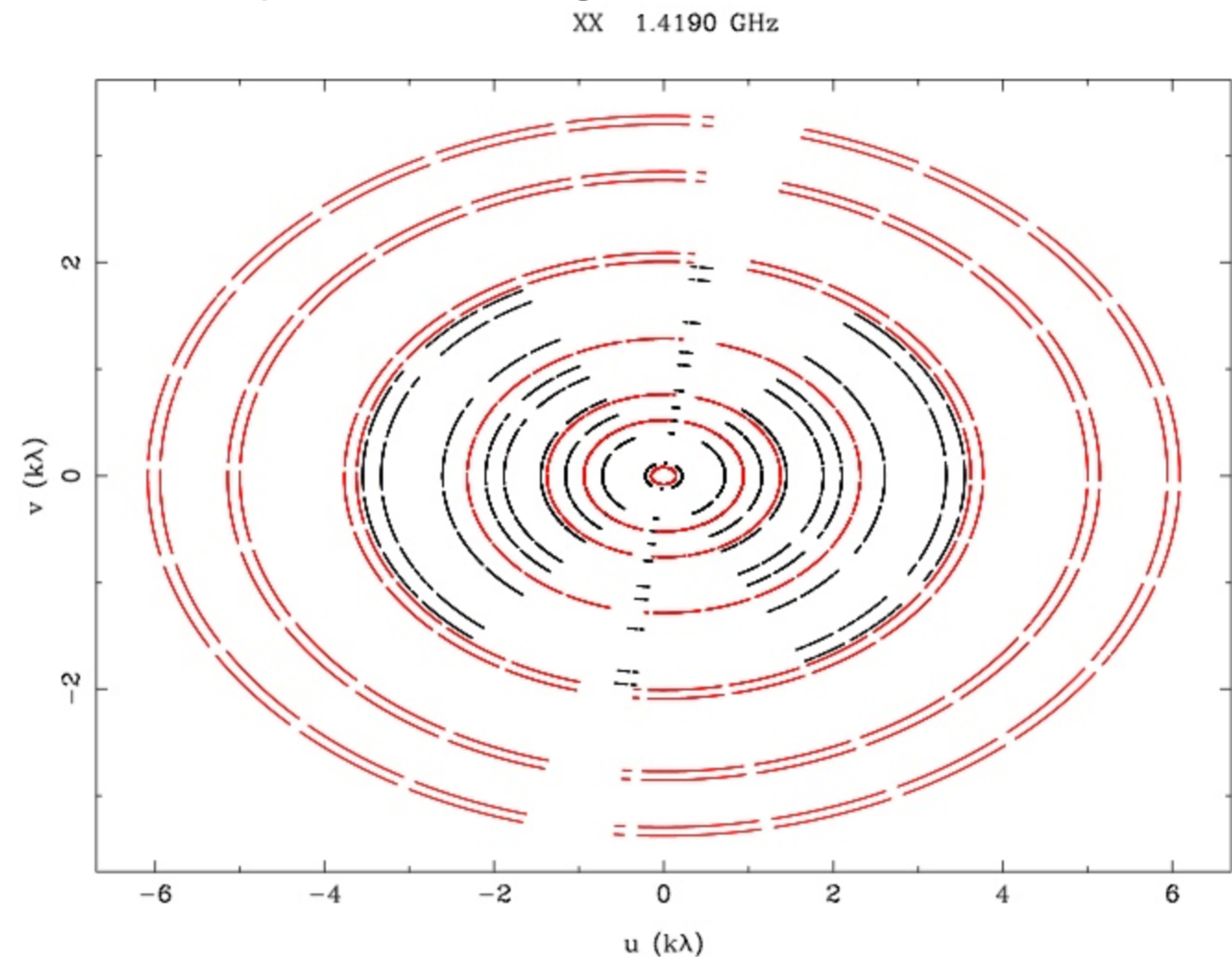


# Earth rotation aperture synthesis

- Let  $u$  be **the east–west component of the projected baseline in wavelengths** and  $v$  be **the north–south component of the projected baseline** in wavelengths.
- During the 12-hour period centered on source transit, the interferometer traces out a complete ellipse on the  $(u,v)$  plane.
- The maximum value of  $u$  equals the actual antenna separation in wavelengths, and the maximum value of  $v$  is smaller by the projection factor  $\sin\delta$ , where  $\delta$  is the source declination.
- If the interferometer has more than two elements, or if the spacing of the two elements is changed, **the  $(u,v)$  coverage will become a number of concentric ellipses having the same shape**.

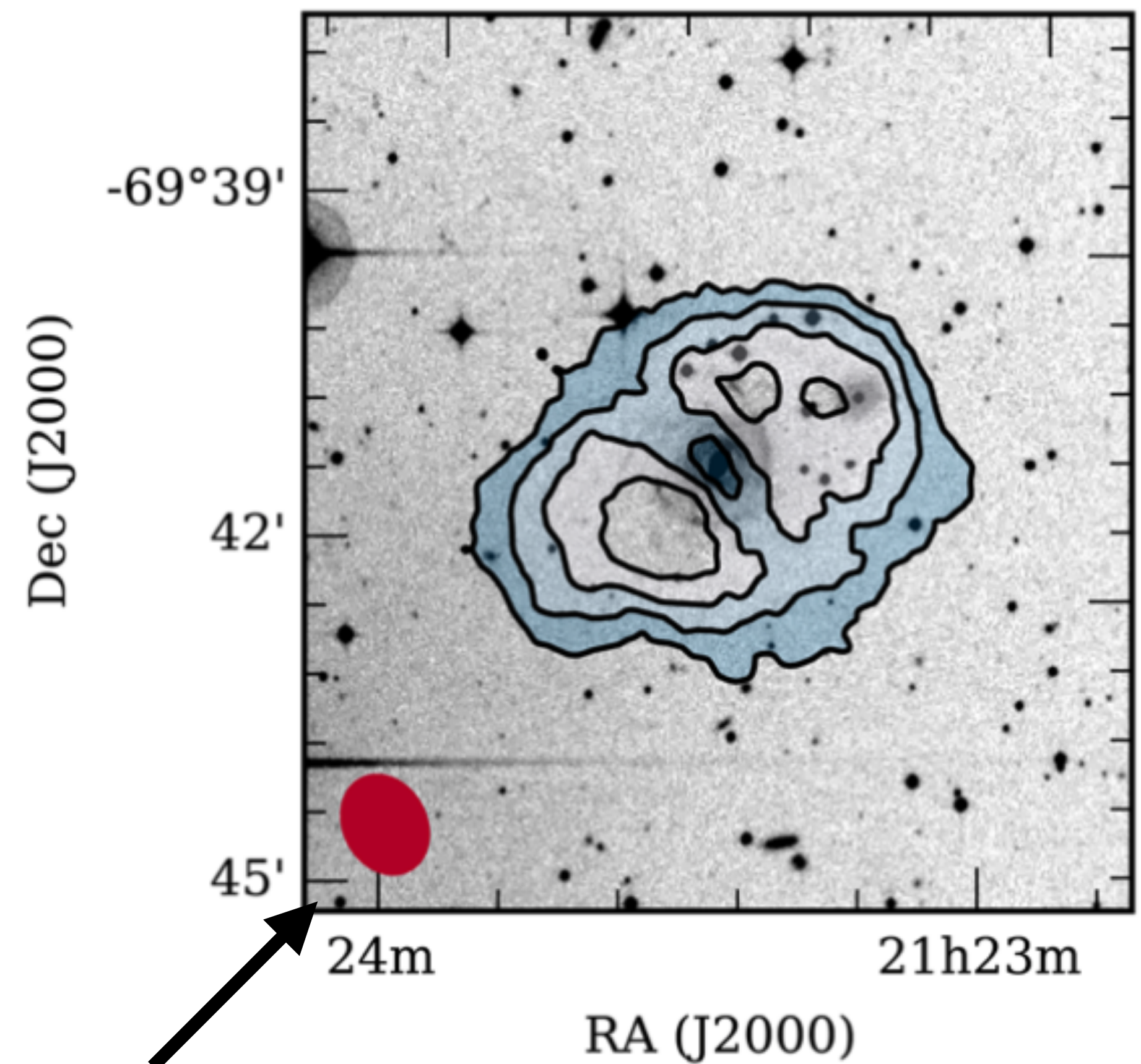


Example uv coverage of ATCA observations



# Earth rotation aperture synthesis

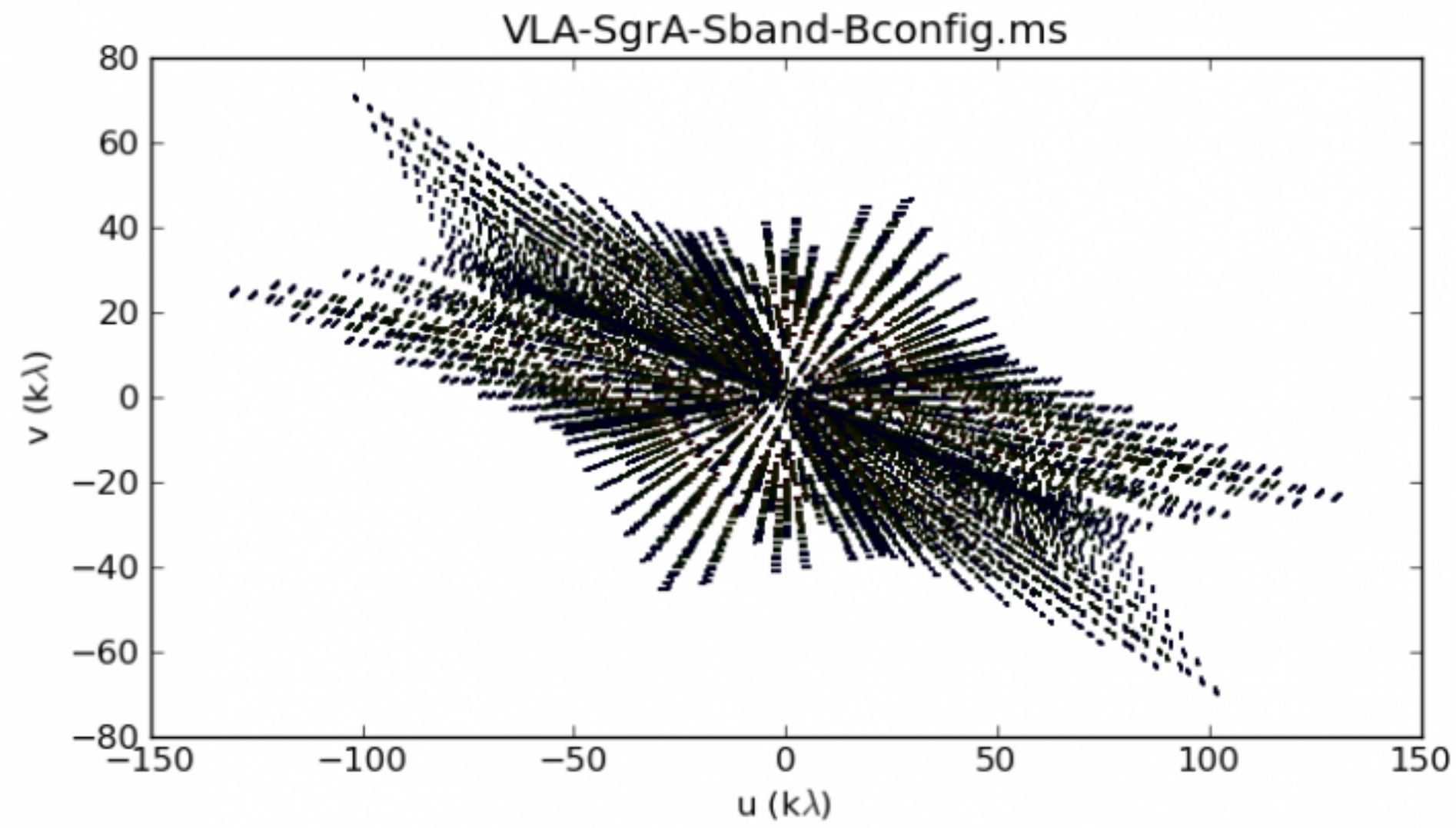
- Thus the **synthesized beam** obtained by east–west Earth-rotation aperture synthesis can approach an elliptical Gaussian.
- The synthesized beamwidth is  $\approx u^{-1}$  radians east–west and  $\approx u^{-1} \csc \delta$  radians in the north–south direction.
- The synthesized beam is circular for a source near the celestial pole, but the north–south beamwidth is very large for a source near the celestial equator.



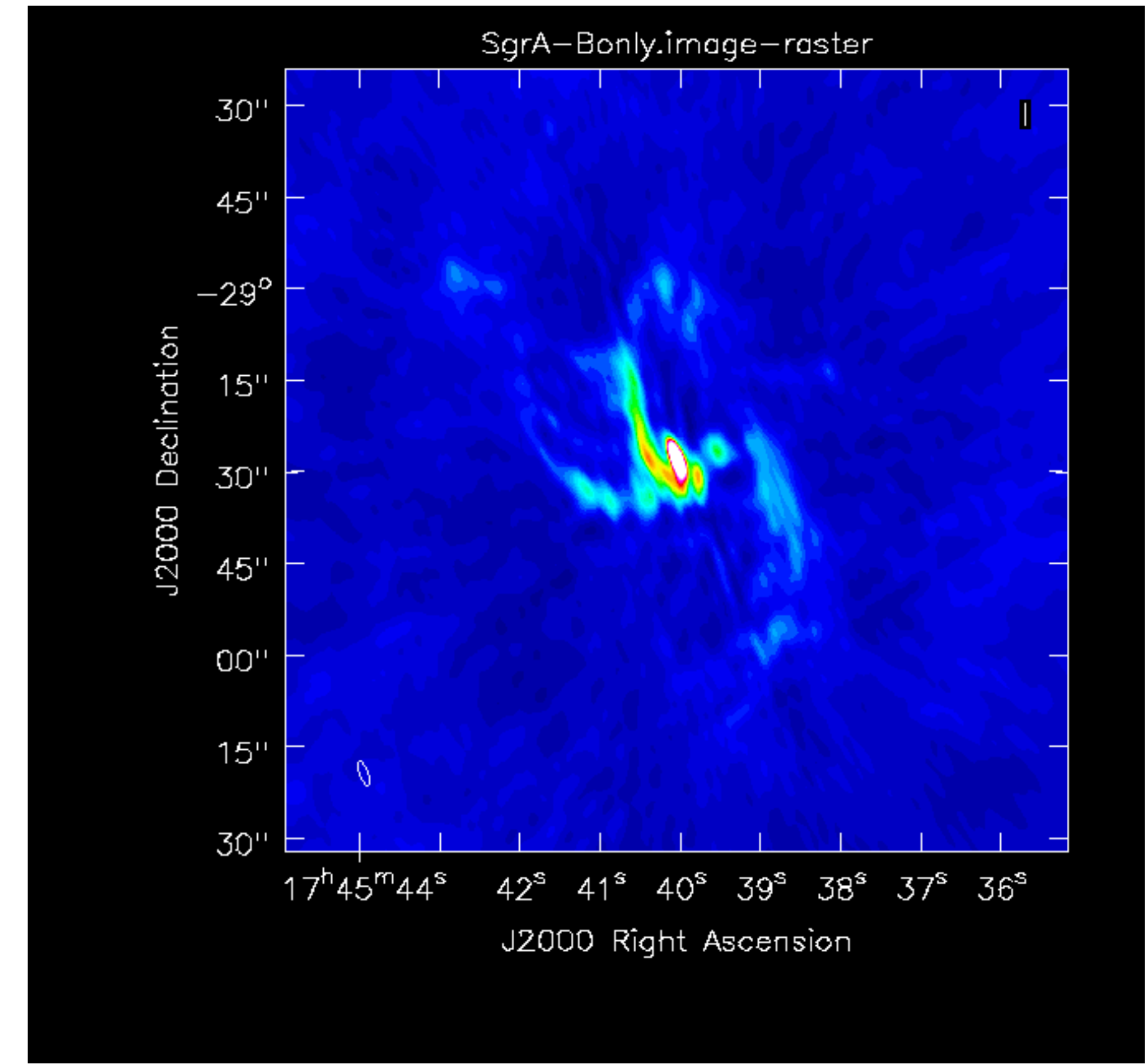
Synthesised beam for neutral hydrogen data of a galaxy

# Earth rotation aperture synthesis

- Non linear arrays, e.g. the Y shaped JVLA fill a 3 dimensional projected volume ( $u$ ,  $v$ ,  $w$ ). Which makes imaging a bit more complicated, but with much better spacial sampling.



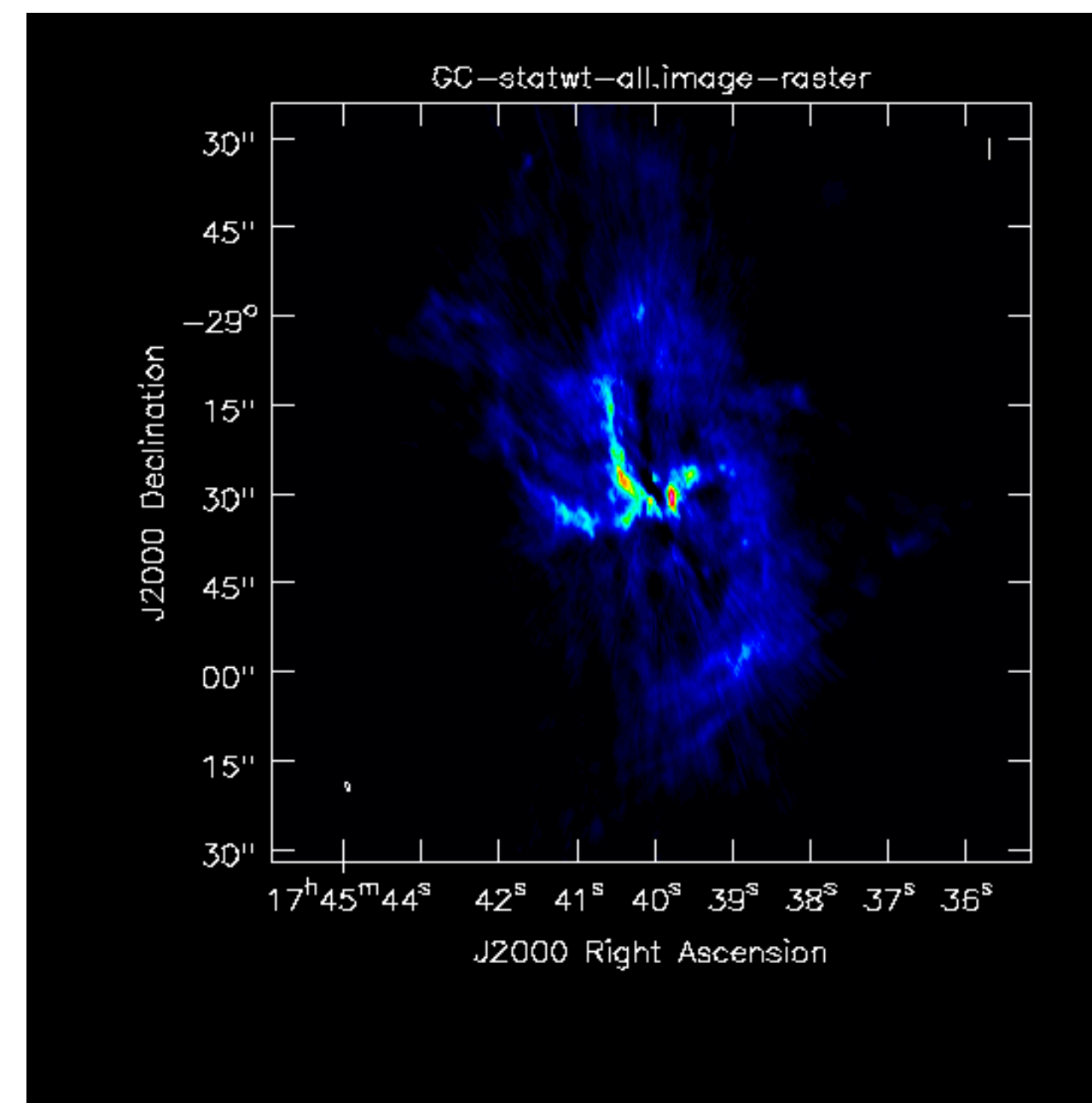
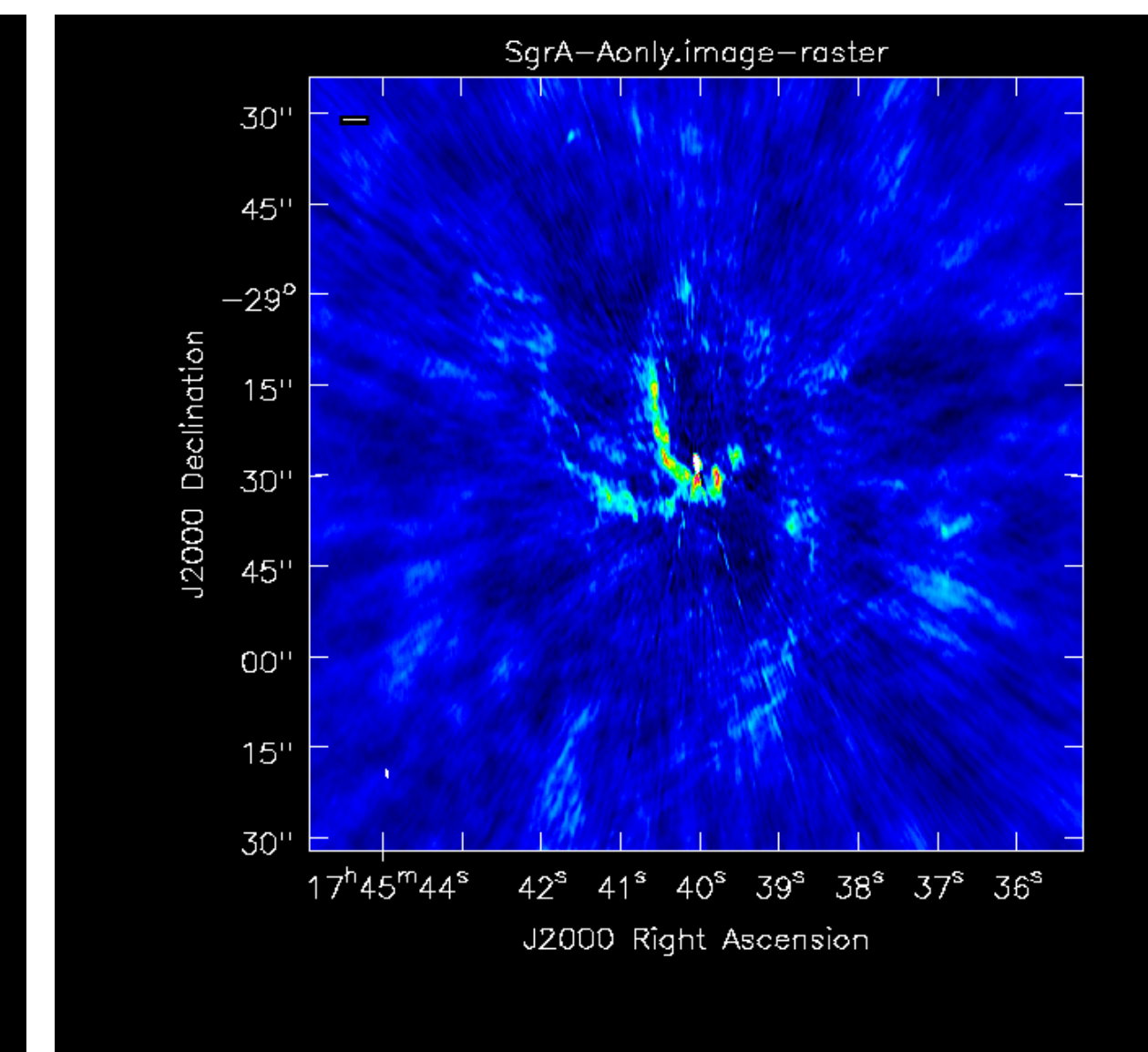
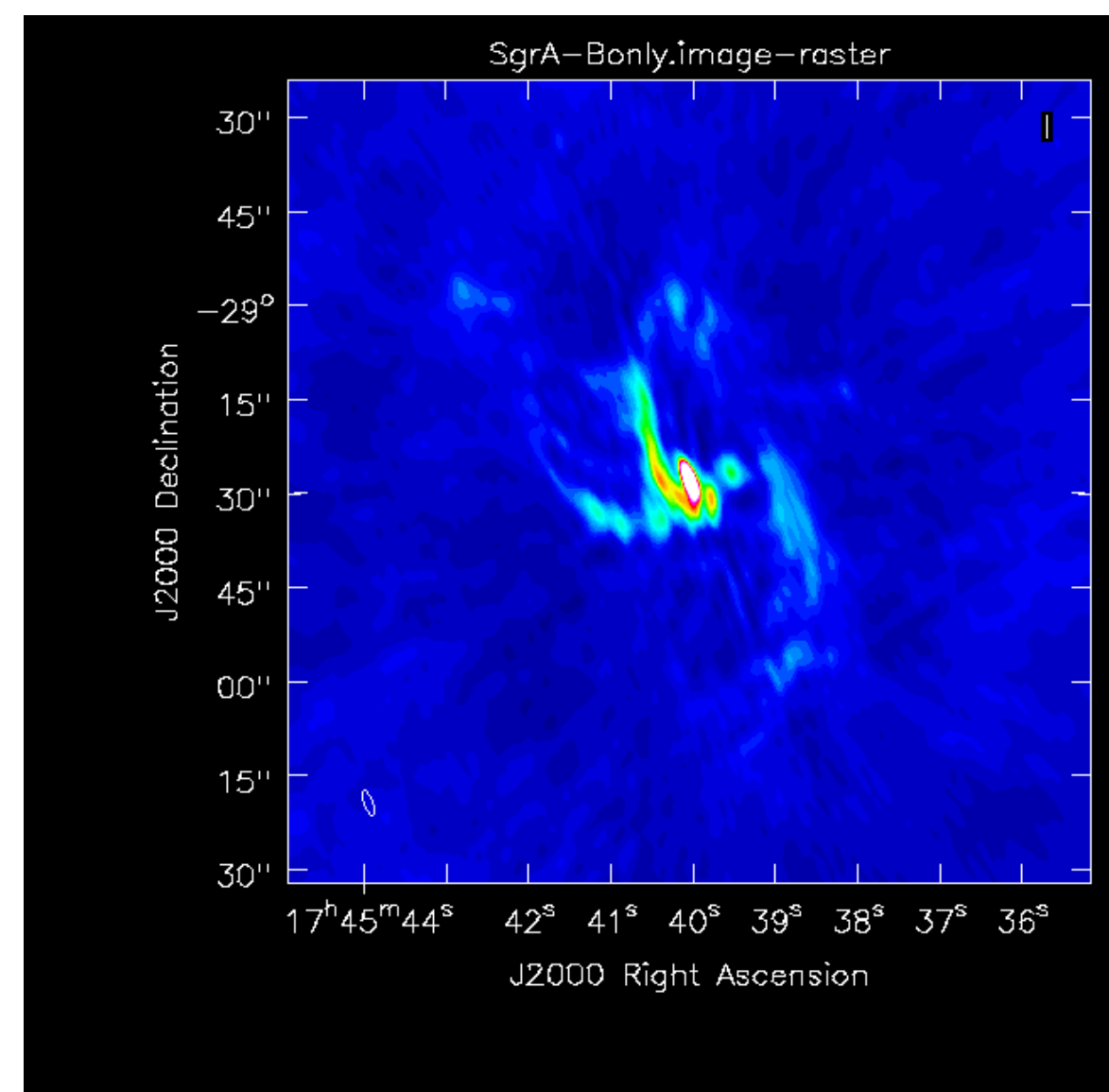
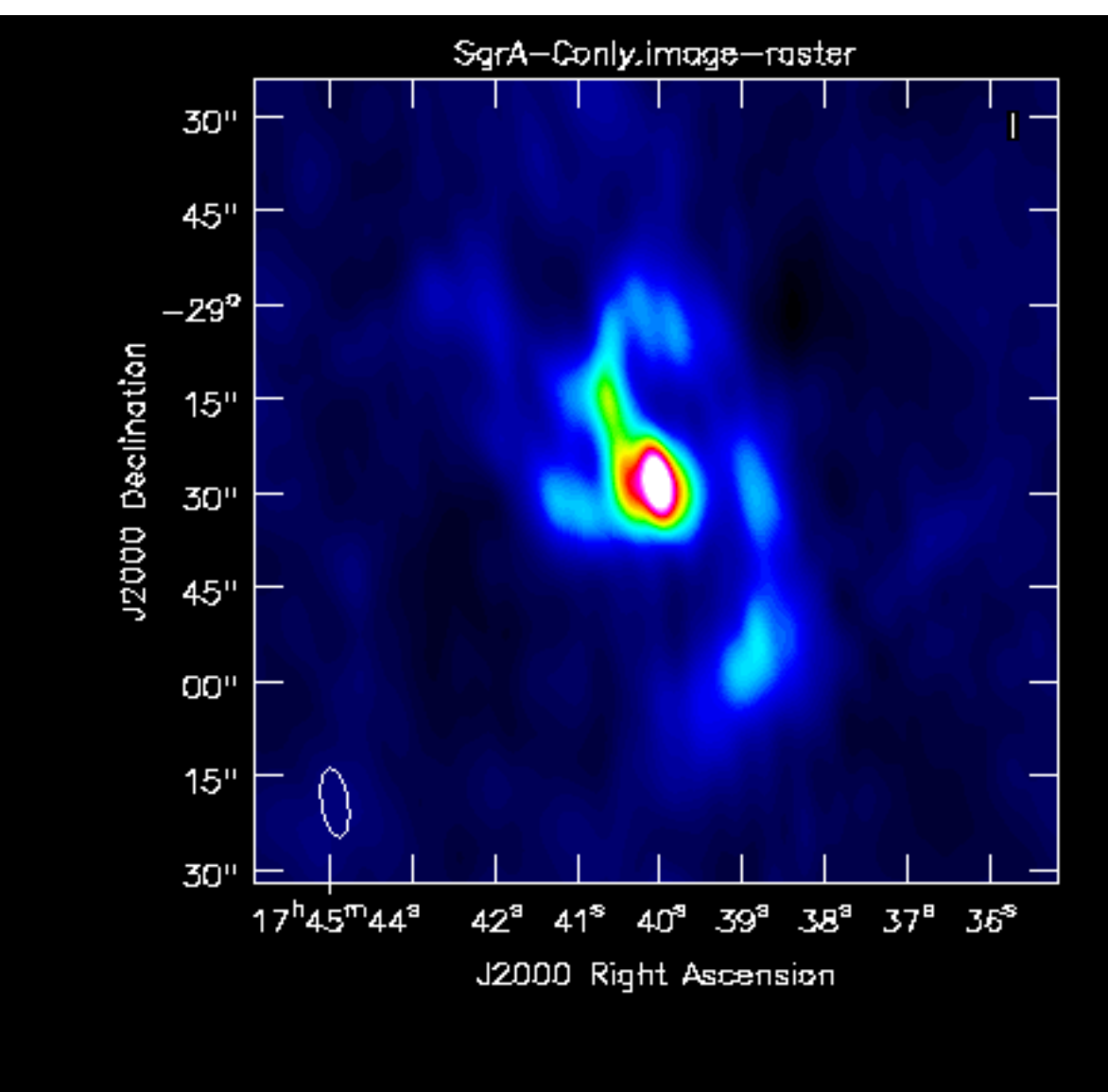
Example uv coverage for VLA observations



The corresponding image of a region in the Galactic Centre.

# Earth rotation aperture synthesis

- The Y shaped JVLA antennas can be moved along railway tracks.
- The different configurations can achieve different spatial resolutions.
- The data from the different arrays can be combined to yield a better image.



3 different array configurations of the JVLA, yield images with different spacial resolution.

The combined image.